



This is to certify that the

thesis entitled

The Influence of Extracorporeal Circuitry On Blood Flow Dynamics During Open Heart Surgery

presented by

William G. O'Neill

has been accepted towards fulfillment of the requirements for

Master_of Science degree in _Mechanical Engineering

Major professo

0-7639

MSU is an Affirmative Action/Equal Opportunity Institution



RETURNING MATERIALS:
Place in book drop to remove this checkout from your record. FINES will be charged if book is returned after the date stamped below.

THE INFLUENCE OF EXTRACORPOREAL CIRCUITRY ON BLOOD FLOW DYNAMICS DURING OPEN HEART SURGERY

bу

William G. O'Neill

A THESIS

Submitted to Michigan State University in partial fulfillment of the requirements for the degree of

MASTER OF SCIENCE

Department of Mechanical Engineering

1983

THE INFLUENCE OF EXTRACORPOREAL CIRCUITRY ON BLOOD FLOW DYNAMICS DURING OPEN HEART SURGERY

bу

William G. O'Neill

Michigan State University

ABSTRACT

Pulsatile roller pumps have been developed recently because of the improved physiological reaction of the body to pulsatile pumping. It is important to understand the effects on the pressure wave from the viscoelastic polyvinyl chloride tubing used to connect patient to pump. A linear bond graph model of the tubing was developed and verified empirically. A linear model of the human arterial system was developed simultaneously which modelled pressure/flow relations in the aorta from a hydraulic impedance viewpoint. Connecting the roller pump and tubing model to the arterial system model permitted evaluation of the effect on the aortic pressure of tubing length, blood temperature, wall thickness and cannula resistance. A low pass hydraulic filter was designed to eliminate high frequency roller pulsations.

TABLE OF CONTENTS

		Page
List of Tables		111
List of Figures		iv
Nomenclature		vii
Chapter 1-	Introduction	1
Chapter 2-	Arterial System Dynamics and Extra-	
	corporeal Circulation	4
	Cardiovascular Ailments and Open Heart	
	Surgery	7
	Pulsatile and Steady Flow Perfusion	9
Chapter 3-	Linear Viscoelasticity	11
Chapter 4-	Experimental Procedure and Parameter	
	Estimation	15
	Resistance	15
	Inertia	19
	Compliance	20
Chapter 5-	Arterial System Model	26
Chapter 6-	Experimental Results	31
	Static Compliance	31
	Dynamic Compliance	35
	Wall Resistance	36
	Temperature Effects	39
	Pulsatile Input Experiment	44
	Extracorporeal Circuit Model	48
	Effect of Changing Tube Length	53
	Effect of Changing Wall Resistance	59
	Effect of Changing Cannula Resistance	59
	Effect of Changing Patient's Compliance	61
	Low Pass Filtering	65

TABLE OF CONTENTS (cont'd)

		Page
Chapter 6 (cont'd)	Manometer Accuracies due to Line	
	Inertial Effects	69
Chapter 7	Discussion	70
Appendix A	A Brief Review of Bond Graph and	
	Eigenvalue Formulation	81
Bibliography		96

LIST OF TABLES

Table #	Title	Page
4.1	Inertia Values for Various Tube Sizes	20
4.2	Tubing Sizes and Materials for Static	
	Compliance Test	21
4.3	Tubing Sizes and Lengths for Step Increase	se
	of Pressure Test	23
5.1	Penn State Arterial Model: Parameter	
	Values	28
6.1	Static Compliance Values (1 ft. Length)	31
6.2	Effect of Number of Elements on	
	Accuracy	35
6.3	Predicted and Actual Frequencies with	
	$C_{\text{dyn}} = 0.0013 \text{ cm}^4 \text{s}^2/\text{kg/ft}$	36
6.4	Natural Freqency and Dynamic Compliance	
	As A Function of Tube Size and	
	Temperature	44
6.5	Tubing Lengths and Areas Resulting in	
	Low Pass Filter	69
A.1	Energy Variables for Various Domains	83
A.2	One Port Variables for Various Domains	83
A.3	Constitutive Equations for Various	
	R1ements	91

LIST OF FIGURES

Figure #	Title	Page
2.1	Diagram of the Heart Including Extra-	
	Corporeal Circulation	· 5
3.1	Maxwell Element	12
3.2	Voigt Element	12
3.3	St. Venant Body	12
3.4	Creep in Voigt Element	13
3.5	Creep in St. Venant Body	13
4.1	Pressure Drop for Various Tubing Sizes	17
4.2	Step Input of Pressure Test Diagram	22
4.3	Experimental Set Up for Pulsatile Test	25
5.1	Arterial System Component Model	27
5.2	Arterial System Bond Graph	28
5.3	Aortic Flow in Mock Arterial System	29
5.4	Aortic Pressure in Mock Arterial System	30
6.1	Measured Pressure Vs. Volume (Compliance)	
	in 3/8"x3/32"x12" Tube	32
6.2	Pressure at End of 2' Tube with a	
	Pressure Step Input	34
6.3	N. Segments of Tubing Represented by	
	an Electrical Analogue	37
6.4	2 ft., 2 Element PVC Tube @ 20° C.	
	(computer output)	40
6.5	Predicted Pressure in Three Foot Tube	41
6.6	Pressure Measured at End of Three Foot	
	Tube with Step Input	42
6.7	Measured Pressure in 2' Tube with	
	Step Input @ 37° C.	45
6.8	Bond Graph for Pulsatile Tubing Test	47
6.9	Two Foot (3/8"x3/32" PVC) Tube with	
	Roller Inputs @ 60 Bpm, 3 1pm	49

LIST OF FIGURES (cont'd)

Figure #	Title	Page
6.10	Predicted Response of Eight Feet of	
	Tubing to Pulsatile Input	50
6.11	Measured Response at End of Two Foot	
	Tube with Pulsatile Input	51
6.12	Pressure Measured at End of Eight Foot	
	Tube with Pulsatile Input	52
6.13	Bond Graph and Component Diagram for	
4.	Two Foot Tube with Mock Arterial System	54
6.14	Aortic Pressure with Two Foot Tube and	
	Roller Input	55
6.15	Effect of Tubing Length on Aortic	
	Pressure	56
6.16	Effect of Tube Length on Volume Flow	
	Rate through the Cannula	58
6.17	Effect of Tubing Wall Resistance on	
	Aortic Pressure	60
6.18	Effect of Cannula Resistance on Aortic	
	Pressure	62
6.19	Effect of Cannula Resistance on Cannula	
	Pressure	63
6.20	Effect of Patient's Arterial Compliance	
	on Aortic Pressure	64
6.21	Low Pass Filtering with Increased	
	Accumulator Compliance	66
6.22	Low Pass Filtering with Increased Inertia	68
7.1	Vena Contracta from Area Change	73
7.2	Cannula Design with Tapered Exit and	
	Pursestring Removal	75
7.3	Extruded Header Tube with 3/4" ID Middle	
	and 3/8" ID Ends	75

LIST OF FIGURES (cont'd)

Figure #	Title	Page	
A.1	Mechanical Oscillator	82	
A.2	Sources and Transformers	84	
A.3	Junctions	84	
A.4	Oscillator Bond Graphs	87	
A.5	Step Input Test Set Up	88	
A.6	Simplified Bond Graph	88	
A.7	Preferred Causality of Elements and		
	Junctions	90	
A.8	Hydraulic Bond Graph with Causality	92	

NOMENCLATURE

_			
P	pressure	E	electrical voltage
V	volume	$Q_{\mathbf{e}}$	charge
V _e	velocity (average)	i	current
Q	volume Flow rate	g	flux linkage
R	resistance	$\mathbf{P}_{\mathbf{m}}$	momentum
С	capacitance	f	flow variable
I	inertance	e	effort variable
c _d	dynamic capacitance	W	eigenvalues
I.D.	inner diameter	Kr	friction factor
1	liters	r	radius
1pm	liters per minute	а	acceleration
bpm	beats per minute	1	length
S	second	m	mass
mmHg	millimeters mercury (pressure)	p	density
kg	killogram	Rent	entrance resistance
cc	cubic centimeters	R	wall resistance
$\mathbf{w}_{\mathbf{n}}$	natural frequency	R ₁	line resistance
N	Newtons	E	ratio damping to critical
lbf	pounds force		damping
m	meters	t	time
rad	radians	Z	phase angle
psi	pounds per square inch	A	area
ft	feet	^A c	area of capacitance
RPM	revolutions per minute	Hz	hertz
k	spring constant		wavelength
N	hydraulic damping	Cacc	Accumulator Compliance
S	stress	400	
е	strain		
ė	strain rate		
L	momentum slug		
F	force		
X	displacement		
x	velocity		

CHAPTER 1

INTRODUCTION

Pulsatile roller pumps have been developed recently because of the improved physiological reaction of the body to pulsatile perfusion during open heart surgery. It is important to understand the effects on arterial pressure and flow from the visoelastic nature of the tubing used to connect patient to pump. Therefore, this thesis will discuss a computer model of extracorporeal circulation developed to understand how varying parameters in the circuit influenced blood dynamics.

Open heart surgery is a procedure which involves completely stopping the heart to treat obstructed coronary arteries, valve disease, and other cardiac ailments. The functions of the heart and lungs are taken over by mechanical devices. Briefly, the procedure bypasses oxygen depleted blood from the vena cavae to an oxygenator where carbon dioxide is exhausted and oxygen taken up. The blood is cooled as it passes through a heat exchanger. A positive displacement roller pump is most commonly used to return blood to the ascending aorta. Pumps in the past have been steady flow, meaning that the rollers rotate at a constant angular velocity. Pulsatile roller pumps better mimic the beating heart by accelerating and decelerating the rollers, thereby creating a pulsatile waveform. The growing acceptance of pulsatile perfusion in the medical community is primarily due to the lower peripheral resistance of the patient reported by many researchers. It is important to know how the viscoelastic characteristics of the polyvinyl chloride tubing affects the pressure and flow waves entering the aorta.

This thesis had two primary objectives:

- to develop a computer model of the viscoelastic tubing,
 and
- 2) to simultaneously develop a computer model of the human arterial system from an overall hydraulic impedance viewpoint.

Once developed and verified empirically, the models could be combined to predict the effect on the aortic wave from changing:

- a) tubing wall thickness,
- b) tubing length,
- c) blood temperature, and
- d) cannula resistance.

Finally the model could be used to design a hydraulic filter to eliminate high frequency pressure fluctuations resulting from rollers engaging and disengaging with tubing in the roller head.

The tubing was modelled as a classical spring, mass, and damper system. The tubing wall incorporated a linear viscoelastic Voigt (Kelvin) element, the parameters of which were determined both empirically and with a computer model.

The overall structure of this report is as follows:

<u>Chapter 2</u> - Cardiovascular dynamics are described with primary emphasis on hemodynamics. A brief review of open heart surgery is presented for readers unfamiliar with the procedure. Finally the rationale for pulsatile perfusion is described.

<u>Chapter 3</u> - A discussion of linear viscoelasticity will introduce the linear Voigt element which will be incorporated in models developed in later chapters. <u>Chapter 4</u> - This chapter explains the analysis, assumptions, and experimental procedures used to identify the inertial, compliance and resistance parameters of the lumped parameter tubing model.

<u>Chapter 5</u> - The Penn State University mock arterial system is modelled mathematically. The procedure for estimating parameter values is explained.

<u>Chapter 6</u> - The experimental results are presented followed by a discussion of results in Chapter 7.

CHAPTER 2

ARTERIAL SYSTEM DYNAMICS AND EXTRACORPOREAL CIRCULATION

Since some readers may be unfamiliar to the workings of the human cardiovascular system and its control, I would like to briefly review the basic principles. Additionally, I believe that it would be useful to outline the components of a typical extracorporeal bypass circuit (extracorporeal means outside the body) with primary emphasis on components which are particularly pertinent to this study: pumps, tubing, and cannulae.

The heart is a four chambered muscular organ which daily beats 100,000 times with a continuous output of 4,300 gallons of blood. 9 Referring to Figure 2.1, oxygen depleted blood returns to the heart via the superior and inferior vena cavae and enters the right atrium with a central venous pressure (CVP) generally around ten millimeters of mercury (mmHg). An internal pacemaker causes both sides (left and right) of the heart to simultaneously contract. Blood initially fills the right ventricle and then is pumped into the pulmonary artery on its way to be oxygenated in the lungs. Blood returning from the lungs to the left atrium has absorbed enough oxygen to replenish the bodies needs and has exhausted carbon dioxide, a metabolic waste product. From the left atrium the blood courses into the left ventricle which then contracts to force blood into the aorta and the rest of the arterial system. The blood pressure in the aorta ranges from a diastolic pressure of 40 mmHg to a peak systolic pressure of 185 mmHg. The heart's ejection fraction is defined to be the percentage of blood ejected during contraction divided by the total volume in the dilated

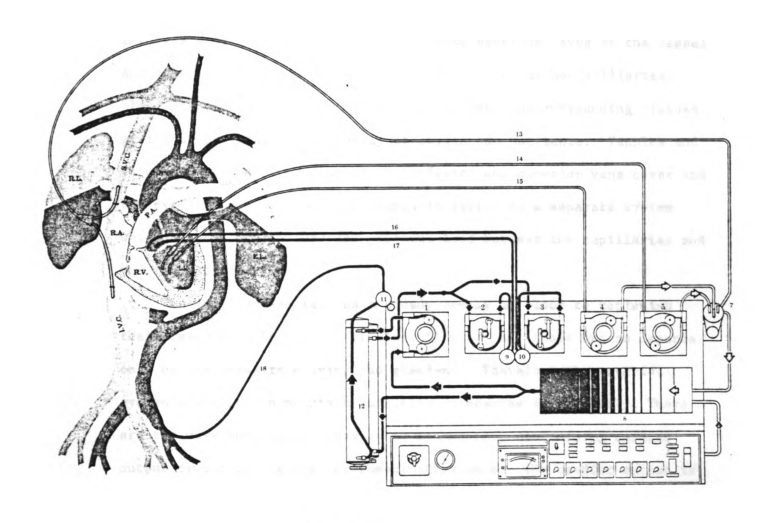


Figure 2.1
Diagram of the Heart with Extracorporeal Circulation

heart and generally is around 50-60%. A "normal" arterial pressure wave would have resting diastolic and systolic pressures of 80 and 120 mmHg respectively with approximately a 40 mmHg differential between the two. Aortic flow rates in a normal pulsatile aorta would be about 5 liters per minute (1pm) in a resting adult. ²⁷ The pressure wave leaving the left ventricle continues down the aorta branching into various arteries with little pressure drop. The transition from arteries to arterioles involves a dramatic reduction in the cross sectional area of the vessel and causes substantial pressure dissipation. From the capillaries, blood diffuses through the vessel's walls into the surrounding tissues giving up the transported supply of oxygen and nutrients. Venules and veins return the blood then to the inferior and superior vena cavae and the cycle resumes again. The lymphatic system is a separate system which returns extra fluid and proteins lost between the capillaries and the interstitial fluid.

The vital organs rely on a steady supply of blood to replenish their reserves. The amount of blood flowing into these organs depends only on the pressure driving the gradient. Therefore the arterial system's ability to maintain sufficient pressures is critical. There are two ways that blood pressure is maintained; controlling cardiac output or increasing the peripheral resistance. The cardiac output is increased simply by speeding up the heart rate as is done during exercise. The systems peripheral resistance consists of the total impedance to flow resulting from head losses due to arteriole size. Sympathetic nerves in baroreceptors in the carotid arteries and the aortic arch send signals to the brain when pressure is too high or low. If pressure is too high, the brain emits a hormonal vasodilator to

increase the arteriole radii. A vasoconstrictor is employed if the pressure falls too low with additional help from fluid being actively pumped into the system from the interstitial fluids. When there is a need for vasoconstriction, a complex chain of events ensues involving two prominent hormones: renin and angiotensin. Angiotensin is a strong vasoconstrictor which seems to require renin for activation.

CARDIOVASCULAR AILMENTS AND OPEN HEART SURGERY

According to estimates by the American Heart Association over 43 million Americans suffer from one form of heart disease or another.

Strokes, heart attacks and other cardiovascular problems are the leading cause of death in this country with the grim responsibility for 51% of all deaths. This is more than twice as fatal as the next leading killer, cancer. To remedy these problems more than 135,000 coronary artery bypass and 35,000 valve operations were performed last year requiring open heart surgery. Since a beating heart is impossible to work on, open heart surgery requires stopping the heart and maintaining the patient's pumping and oxygenation functions mechanically. The traditional components of open heart surgery are diagrammed in Figure 2.1 and include:

- Oxygenators Most oxygenators provide a large blood to air surface area to facilitate diffusion of oxygen into the blood and carbon dioxide out. Many have built in heat exchangers to cool the blood. Hypothermia reduces the metabolic demands of the body during surgery.
- 2) Pumps The most common pump in use today is the positive displacement roller pump. Recently pulsatile roller pumps have been introduced to replace the traditional steady flow

pumps. These pulsatile pumps accelerate the rollers to a steady velocity very quickly, maintain that velocity for the course of the pulse width, and then provide rapid braking to stop the pump head. A typical duty cycle might be for the pump to be on for one half second then off for one half second.

- 3) Filters These trap small particulates and break up fine air bubbles. Additionally they catch potentially fatal large air bubbles which can then be bled out of the filter. Filters will not be discussed in this report.
- 4) Tubing Polyvinyl chloride (PVC) and silicone rubber are the two most common materials used in tubing because of their translucence, flexibility and gentleness to blood.
- 5) Cannulae Cannulae act as a nozzel to direct flow from the extracorporeal circuit into and out of the patient's circulatory system.

Other elements of surgery of less concern to this study are cardioplegia delivery systems, suction and vent pumps, blood chemistry analyzers, temperature displays and various safety equipment.

Cardioplegia is a very cold chemical solution which blocks the electrical conduction in the heart. The combination of cold plus the chemical blockers causes the heart to stop. Suckers and vents remove blood from the operated area. Blood chemistry generally requires removing a blood sample from the oxygenator periodically and sending it down to a central laboratory. Oxygen saturation, degree of clotting, acidity, etc. are all reported back to the operating room.

PULSATILE AND STEADY FLOW PERFUSION

Since the start of open heart surgery, the benefits of pulsatile vs. steady flow pumping have been debated. Traditionally perfusionists utilized constant angular speed pumps because they were simple. In recent years a growing body of papers have noted the desirability of more closely mimicking the heart. At the same time the technology required to pulse a roller pump head was being developed.

Some of the benefits of pulsatile pumping include decreased peripheral resistance, better organ perfusion, improved lymph flow, decreased post operative hypertension, and a better ejection fraction from the restarted heart. Papers reporting decreased peripheral resistance with pulsatile perfusion were written by Mandelbaum et al., ¹² Mavroudis, ¹⁴ Angell et al., ¹ and Taylor et al. ²⁵ Taylor explained this phenomenon by noting higher plasma levels of angiotension II during steady flow perfusion than with pulsatile pumping. Watkins et al. 28 reported higher plasma concentrations of another vasoconstrictor, thromboxane, during steady flow. Burton and his colleagues found that vasomotor nerves in the arterioles which controlled the degree of vasoconstriction were sensitive to increases in the frequency of stimulating impulses. The baroreceptors sending the impulses were found to be sensitive to the form and amplitude of the pressure wave (Mandelbaum) 12. Soroff et al. claimed that the nerve impulses arising in the receptors are "a function of the rate of change of pressure as well as the absolute level of pressure and stretch."23 The body seems to view steady flow perfusion as a crisis condition since the baroreceptors are not being properly stimulated and reacts as if there was excessive fluid loss by constricting the arterioles.

Mavroudis demonstrated better kidney function, lymph flow, and oxygen consumption during pulsatile pumping. 14 Clarke reported better liver function and several researchers have commented on better brain perfusion. 5 Landymore et. al. studied twenty patients undergoing coronary artery bypass surgery and divided them into two groups with all treatment being identical except that the control group received steady flow perfusion while the second group was pulsatile. 10 This study reported hypertension (defined as having pressures of 180/100 mmHg) after surgery in 80% of the steady flow patients versus 20% of the pulsed patients. He found that the non-pulsed patients had more renin stimulation than the other group.

CHAPTER 3

LINEAR VISCOELASTICITY

Many biological materials and polymers possess characteristics unlike many other materials common to engineering applications. Conventional elasticity theory cannot be applied to these materials because linear elastic theory assumes that a small strain or deformation results from an applied stress. This assumption is incompatible with highly deformable substances such as rubber, polyvinyl chloride, and arterial walls. Elastic materials also will return to an undeformed state once the stress is removed. Polymers on the other hand tend to exhibit "memory" and will deform permanently if a stress is applied for a sufficiently long time. Viscous fluids are similarly incapable of recovering from an applied stress. Hence polymers and biological tissues possess characteristics common to both elastic and viscous materials and are consequently dubbed viscoelastic materials. Although many of the substances in question are inherently nonlinear, some linearization techniques will be applied so that these materials can be treated as linear under limited conditions.

Viscoelastic behavior is conveniently described by a combination of two elements: the linear massless spring and the linear dashpot.

Stress applied to a spring with a constant "K" will yield a deformation defined by the relation:

S = K e EQN. 3.1

where S is the stress and e is the strain. The analoguous equation

relating strain rate, e, or flow to the stress is:

$$S = N \stackrel{\bullet}{e}$$
 EQN. 3.2

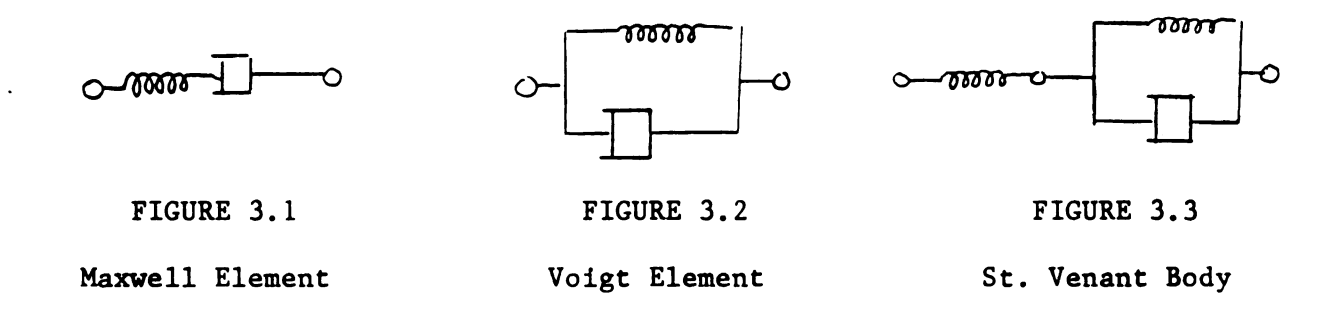
where N is the value of the viscous damping of the dashpot.

Two basic combinations of these elements are the Maxwell element with the spring and dashpot in series (Figure 3.1), and the Kelvin or Voigt model using a parallel arrangement (Figure 3.2). The stress-strain relation for the Maxwell element is:

$$\frac{S}{K} + \frac{\dot{S}}{N} = e$$
 EQN. 3.3 and
$$S = K e + N \dot{e}$$
 EQN. 3.4

for the Voigt model. 13

These models are limited in their ability to accurately describe actual behavior of physical systems.



The Maxwell element will yield continuously with an applied load because of the viscous element. For this reason the Maxwell element is probably best applied to viscoelastic fluids. The Voigt element cannot respond

instantaneously to the load because the viscous element induces a phase lag with the load. The Voigt element will elongate only to a finite length which is dictated by the spring constant. For this reason Westerhof claims that it has been used more frequently than the Maxwell model to represent living materials. The limitation of both models led to a modification consisting of a spring added in series with the Voigt element. This St. Venant body is diagrammed in Figure 3.3.

The benefit of the St. Venant body over a Voigt element can be shown by examining the response of both to an instantaneously applied force. Since the dashpot retards the elongation of the spring, the length will increase exponentially towards a finite length. This phenomenon, known as creep, is shown in Figure 3.4 and 3.5 for the Voigt and St. Venant models respectively. The St. Venant body is able to respond instantly because of the series spring but then the lengthening proceeds like the Voigt model.

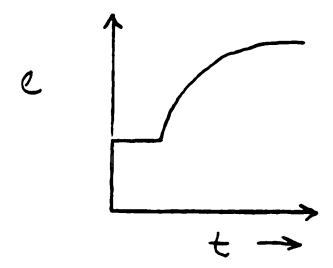


FIGURE 3.4

Creep in Voigt Element

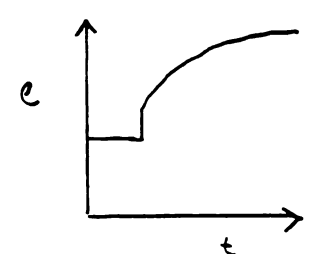


FIGURE 3.5

Creep in St. Venant Body

The Voigt model was used to model the wall of extracorporeal tubing for several reasons. First, the simplicity of the model would facilitate the construction of multi-element, lumped parameter models.

Secondly, because only one spring constant and one damping coefficient would need be identified, parameter estimation would be simpler for this model than for the St. Venant body. Finally, the computer program used to integrate the state equations is limited in the number of state variable it could handle. Each storage element (I or C elements) would yield a state variable, so therefore, the extra spring in the St. Venant body would require half again as many state variables per unit length as the Voigt element. This in turn would limit the number of segments and would require that each segment be longer. It was felt that the benefits of using the St. Venant model would not outweigh the disadvantage of needing larger segments.

It would be possible to continue discussing viscoelasticity and the research done on arterial viscoelasticity ad infinitum, but a complete discussion of linear viscoelasticity is not the objective of this report. Additionally, much of the literature focuses on arterial viscoelasticity which may or may not be applicable to tubing materials. I would therefore like to finish this section with the results of one particular experiment by D. H. Bergel on the static and elastic properties of arterial wall since it will later apply to the tubing problem. Bergel found that the static compliance of an excised arterial segment in vitro, differed from the value determined under dynamic conditions. He found that the ratio of the dynamic Youngs modulus versus the static modulus ranged between 1.1 and 1.7 depending on the amount of muscle in the arterial wall. Youngs modulus is inversely proportional to the compliance of the tubing or wall so a higher Youngs modulus translates into lower compliance.

CHAPTER 4

EXPERIMENTAL PROCEDURE AND PARAMETER ESTIMATION

A segment of tubing was modelled as a spring, mass, and damper system where the inertia of a segment of fluid represented the mass. The springiness of the PVC tubing wall was modelled with a Voigt viscoelastic compliance element as discussed in Chapter 3. The damping analogue in a segment of tubing was comprised of two linear resistance elements: line resistance (R_1) due to viscous fluid shearing and wall resistance (R_2) in the Voigt element. The value for hydraulic inertia is a calculated quantity while C, R_1 , and R_2 were determinted experimentally.

Some of the assumptions made in this model were:

- Blood is an incompressible, homogeneous and newtonian fluid and, in fact, water can be used as an analogue. Although incompressibility is not an unreasonable assumption, homogeneous, newtonian fluid can be rationalized only if one is not concerned with velocity differentials across the cross section. In this study, average velocities and pressures will be solved for.
- 2) The mass in the control volume is constant.
- 3) Flow is one dimensional.
- 4) There is no change in tube length with time.

RESISTANCE

The resistance element R_1 , is the hydraulic dissipation which will cause a pressure drop P, for a given flow rate Q:

If we consider the pressure drop due to viscous line losses, Poiseuilles equation for laminar, steady flow predicts that the pressure drop will be inversely proportional to the radius of the tube to the fourth power or:

$$^{P} \propto \frac{1}{r^4} Q$$

Because this equation is valid only for laminar, steady flow, it can not be applied to the immediate problem of pulsatile flow which may occasionally be turbulent. The value for the resistance can be determined experimentally. Small pitot tubes were tapped into a tube with steady, fully developed fluid flow. The height of the water column in the pitot tubes was measured at regular intervals. The pressure drop per unit length for various flow rates is shown in Figure 4.1. This figure is from a textbook, but nearly identical results were found at Sarns R & D Laboratory. Most tubing used during open heart surgery has a 3/8" or 1/2" inner diameter (3/8" ID is the most common size and used in all subsequent tests in this report). The slope of P vs. Q in Figure 4.1 can be linearized over the flow range of 2-6 1pm without much error. The linearized resistances over this range for 3/8" and 1/2" ID's are equal to 2 mmHg/lmp and 0.5 mmHg/lmp respectively. These units are converted to units of kg, cm, and seconds. A conversion which will be useful is:

$$1 \text{ mmHg} = 1.332 \text{ kg/cm s}^2$$

Line resistances are:

$$R_1(3/8") = 0.16 \text{ kg/cm}^4$$

 $R_1(1/2") = 0.04 \text{ kg/cm}^4$

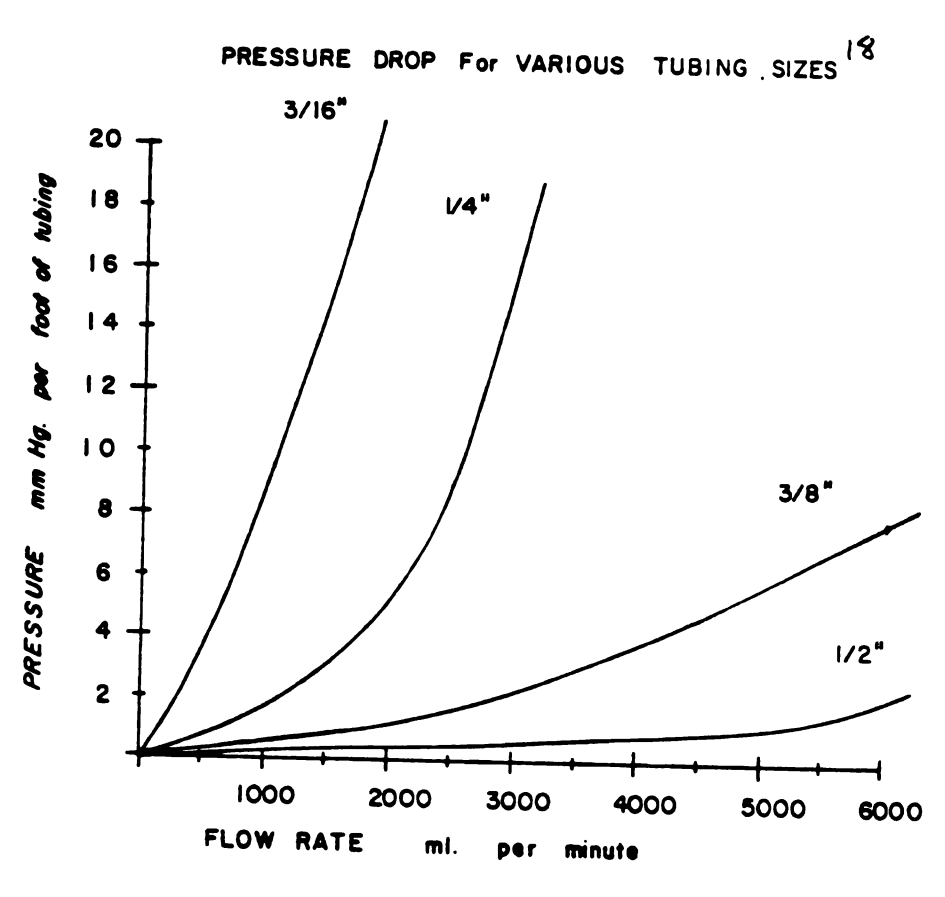


Figure 4.1

Estimating the value of turbulent losses or losses due to T-junctions, sudden contractions/enlargements, valves, etc. can be estimated by introducing a loss coefficient K_r . This is a dimensionless constant determined empirically or obtained from engineering handbooks. K_r is introduced into the energy equation for steady laminar flow through a control volume in a tube:

$$P_1 - P_2 = K_r p V_e^2/2$$
 EQN. 4.1

where p is the density of the fluid and V_e is the average velocity across the cross section. This nonlinear equation for the resistance can be linearized over a limited range of flows by eliminating higher order terms in the Taylor series expansion. If the velocities of interest are within a nominal operating range, the Taylor series expansion would reduce equation 4.1 to:

$$P_1 - P_2 = P_0 + \frac{dP}{dV_0}$$
 (V_e - V₀) EQN. 4.2

where \mathbf{P}_0 and \mathbf{V}_0 are nominal operating points. For a fairly rough approximation the operating points can be assumed to be zero and equation 4.2 reduces to:

$$P_1 - P_2 = K_r p V_e$$

Frictional resistances resulting from entrance effects from the reservoir to the tube, in the step input pressure test (to be discussed later) can be estimated using the loss coefficient:

$$K_{\mu}(entrance) = 0.5$$
 (FROM REF. 3)

Using the linearized resistance developed previously:

$$R_{\text{entrance}} = K_r p = 0.5(0.001) = 0.0005 \text{ kg/cm}^4$$

INERTIA

Finding the hydraulic inertia of a volume of fluid requires starting with Newtons second law:

$$F = m a$$

Dividing each side of Newtons equation by the area will give:

$$\frac{\mathbf{m}}{\mathbf{P} = \mathbf{A} \mathbf{a}}$$
 EQN. 4.3

But the acceleration of a fluid is simply the rate of change of the cross sectional velocity which can be related to the rate of change of the volume flow rate by:

$$a = dV_e/dt = d(Q/A)/dt$$

If the area does not change with time, A can be taken out of the derivation. Thus:

$$\frac{m}{P = A^2} \frac{dQ}{dt}$$
 EQN. 4.4

The mass can be more conveniently described in terms of the volume times the density:

$$m = V p = A l p$$
 EQN. 4.5

Substituting this value for the mass into equation 4.3 gives the final relation for pressure in terms of the rate of change of the volume flow.

$$\begin{array}{c|cccc} p & 1 & dQ \\ P & A & dt & EQN. & 4.6 \end{array}$$

Inertia relates an effort to the rate of change of the flow and so consequently the hydraulic inertia can be described as:

$$\frac{p \, 1}{P = I \, dQ/dt \text{ where } I = A}$$
 EQN. 4.7

Hydraulic inertias have been computed directly in Table 4.1

TABLE 4.1

	Inertia Values	for Various Tube Si	zes*
I.D.	Area	Length	I
inches (cm)	cm²	inches (cm)	kg/cm ⁴
3/8" (0.95)	0.714	6" (15.24)	0.0214
3/8" (0.95)	0.714	12" (30.48)	0.0428
1/2" (1.27)	1.27	6" (15.24)	0.012
1/2" (1.27)	1.27	12" (30.48)	0.024

 $* p_{H20} = 0.001 \text{ KG/CC}$

COMPLIANCE

Hydraulic compliance is probably the simplest of all the variables to define. The hydraulic compliance is:

C = V/P EQN. 4.8

This is as far as we need go to derive the hydraulic compliance.

An evaluation of the wall tubing compliance and resistance required a test which should isolate only the desired variable. A static compliance test was devised so that only the wall compliance could be evaluated. A fixed volume of fluid was injected with a graduated syringe into a tube with a pressure transducer plugging the distal end. The slope of the volume vs. measured pressure would be the static compliance. Ideally this value would be identical in the dynamic case even though Bergel reported discrepancies between static and dynamic compliances. Once the compliance was known, a second test subjected a length of tubing to a step pressure increase. The damping envelope resulting from the transient step or the time constant for an overdamped

system would be used to identify the only unknown resistance—the wall resistance. This experiment would be repeated for several different tubing lengths to verify the results obtained in the initial test. At this point the tubing model could be extended to have a source of flow coming in from a pulsatile pump. The model could be extended so that the flow was being directed from the tubing into a model of the human arterial system so that the aortic pressure could be determined for various tubing conditions.

A Microswitch, strain gauge type, liquid pressure transducer was calibrated against a column of mercury before each day's testing. The natural frequency of the device was reported by the manufacturer to be 1 kHz which was substantially higher than any frequency expected in this procedure. The manometer's output was recorded with a PDP-11 microcomputer made by Digital Equipment Corp. All flows were measured with a Narco flow transducer of the inductance type.

Static compliance tests were performed on the tubing sizes and types listed in Table 4.2. All lengths were 12 inches.

TABLE 4.2

Tubing Sizes and Materials for Static Compliance Test

Material	<u>I.D.</u>	Wall
PVC (Tygon)	3/8"	3/32"
PVC	3/8"	1/16"
Silicon	3/8"	3/32"
PVC	1/2"	1/8"
PVC	1/2"	1/16"

The tubing sizes listed in Table 4.3 were tested with the step pressure test of experiment two. This test is shown in Figure 4.2 and a detailed development of the differential equations for this system is found in Appendix A. A length of fresh tubing was filled with tap water, purged of air, and pressurized to around 80 mmHg (corresponding to diastolic pressure) while attached to the reservoir. A pressure transducer plugged the far end. The tubing was clamped off manually with a hemostat and the reservoir was pressurized to a higher value of 120 mmHg to correspond with systolic pressure. Pressures were recorded by the DEC PDP-11 computer when the hemostat was quickly released. The tubing experienced a step input of pressure. Tubing was tested at both room temperature (20°C) and around body temperature (37°C) to determine the effect of temperature on the contractile characteristics.

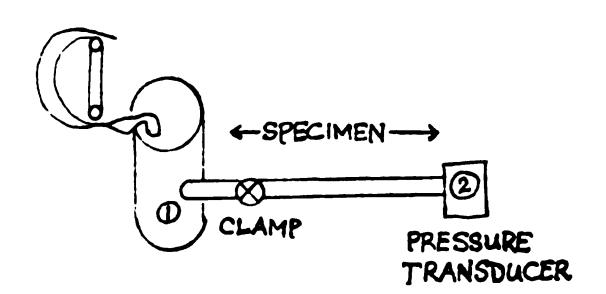


FIGURE 4.2
Step Input of Pressure Test

TABLE 4.3

Tube Sizes and Lengths for Step Increase of Pressure Test

I.D.	WALL	LENGTH	TEMPERATURE
Inches	Inches	Inches	°C
3/8	3/32	24	20
3/8	3/32	24	37
3/8	1/16	24	20
3/8	1/16	24	37
3/8	3/32	36	20
3/8	3/32	48	20
3/8	3/32	96	20
1/2	3/32	36	20
1/2	3/32	36	37

The final test before the model was used with a modelled arterial system involved running the pulsatile pump at a fixed pulse rate (in beats per minute, bpm), a fixed flow rate (lpm), and a baseline of zero. The baseline means that between pulses the pump head comes to a complete stop. The tubing in the head of the pump (known as the header) was of a fixed length. The pump was run at 3 liters per minute and 6 liters per minute with a half inch tube in the head because this would cause the rollers to stop in exactly the same spot if the pulse rate was fixed at 60 bpm. This was important because if the roller did not stop at the identical position with each cycle, the tubing compliance would be a function of where the roller head stopped and therefore would be continually varying. Even with the pump head pulsed at this artificially fixed rate, the tubing compliance varied with the roller

position when the rollers were in motion making an absolute determination of the behavior of the system an impossibility. For this reason some of the data may not correlate well with the computer prediction of the system's behavior. This discrepancy was not felt to be a problem since the qualitative effects of changing tubing parameters and patient parameters were considered to be more important than the quantitative evaluation of this particular physical situation. words, the effect of using seven feet of tubing rather than ten on the pressure wave in the aorta was more important than developing a model which exactly replicated the behavior of a pump running at 3 lpm, 60 bpm with a fixed length of tubing. The final pulsatile test was run with tubing lengths of two and eight feet and an approximate header length of about eight inches. A ball valve was placed in the line downstream of the tubing with pressure transducers measuring pressure on either side of this hydraulic resistor. A Narco flow meter tracked the flow so that the value of the resistance (pressure drop divided by flow rate) could be determined. The resistor was evaluated with the pump running at a steady flow rate of three liters per minute. Flow leaving the resistor entered a storage reservoir which had a constant pressure internally. Flow exited from the other side of the reservoir into the suction end of the pump. The diagram for this system is shown in Figure 4.3.

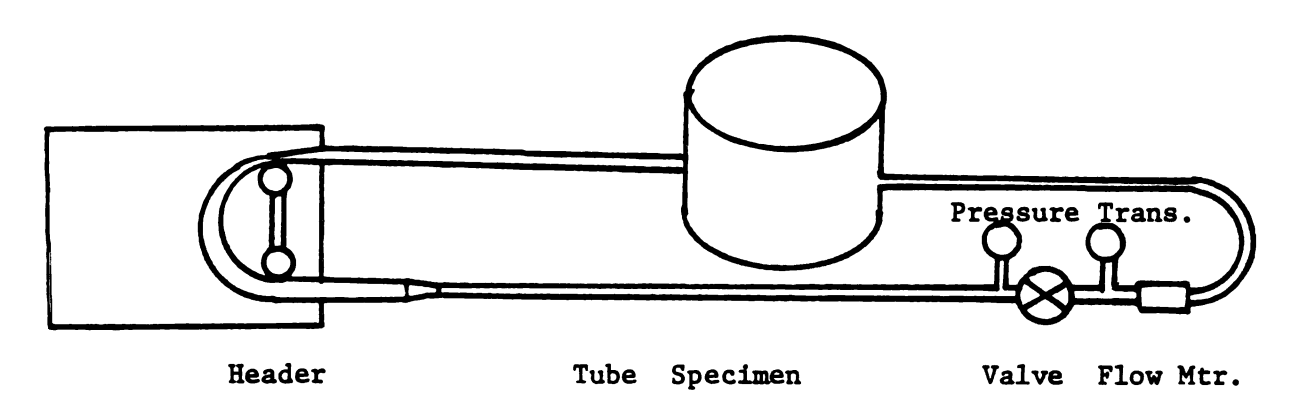


Figure 4.3
Experimental Set Up for Pulsatile Test

CHAPTER 5

ARTERIAL SYSTEM MODEL

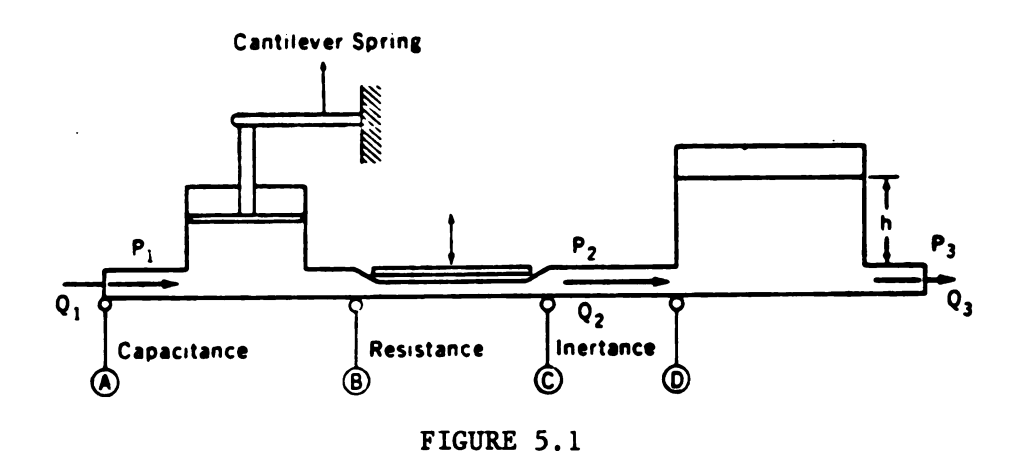
Proper evaluation of pumps, tube sets, cannulae and other components of extracorporeal circulation requires either extensive animal testing or reasonable laboratory models of the arterial system; either hydromechanical or digital. The testing on animals is far too expensive to be used on a routine basis, so therefore useful models must be developed and employed. The model must satisfy the following criteria:

- The system must provide an accurate analog of the cardiovascular system from an overall hydraulic impedance point of view.
- The system must have readily adjustable resistance and compliance elements so that various physiological conditions can be simulated.
- 3) The system must be easy to operate.

A mock circulatory system was developed for use in testing artificial hearts by researchers at Penn State University in 1971. 19

Due to the wide acceptance, good performance, and detailed documentation which facilitated construction of the model, a similar device was developed for use in the R & D laboratory at Sarns. This section will describe not only the hydromechanical model, but also the bond graph computer model which permitted use with the tubing computer model. The system is diagrammed in Figure 5.1 with capacitance, resistance, and inertance elements in series. The bond graph for this system is shown in Figure 5.2 with a flow input coming from the left ventricle and a

source of effort modelling the relatively constant central venous pressure (CVP) at the vena cavae. It was assumed that all compliance came from the accumulator, resistance from the two plates squeezing a bed of flexible tubes, and inertance from the fluid in the line between C and D.



Arterial System Model 19

The first inertia in the bond graph (I_2) is an activated bond used as a pressure tap to measure the aortic pressure. The bond graph for this system yields the following coupled differential equations:

$$L_2 = 1/C V_3$$
 $V_3 = S_{f1} - 1/I_6 L_6$
 $L_6 = R/I_6 L_6 + S_e + 1/C V_3$

The values for R, C, and I_6 (I_2 is set to the arbitrary value of 1 since it does not affect the system dynamics) were found by introducing a flow as close as possible to the flow coming from the left ventricle and varying the parameters until a physiologically correct aortic pressure was obtained. The results found by the Penn State team were listed in Table 5.1

TABLE 5.1

Penn State Arterial Model: Parameter Values

 $R = 1.81 \text{ kg/cm}^4$

 $C = 0.5 \text{ cm}^4 \text{s}^2/\text{kg}$

 $I = 0.021 \text{ kg/cm}^4$

A flow rate shown in Figure 5.3 was input to the model and the resulting aortic pressure wave predicted by the computer is shown in Figure 5.4.

The flow and pressure wave for the computer model of the Penn State arterial analogue are in fair agreement with flows and pressures measured in the human arterial system. It is, of course, a fairly gross model of a very complicated system but will be useful in identifying trends induced by changing parameters.

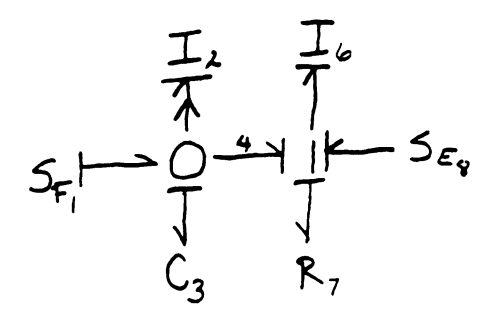


FIGURE 5.2

Arterial System Bond Graph

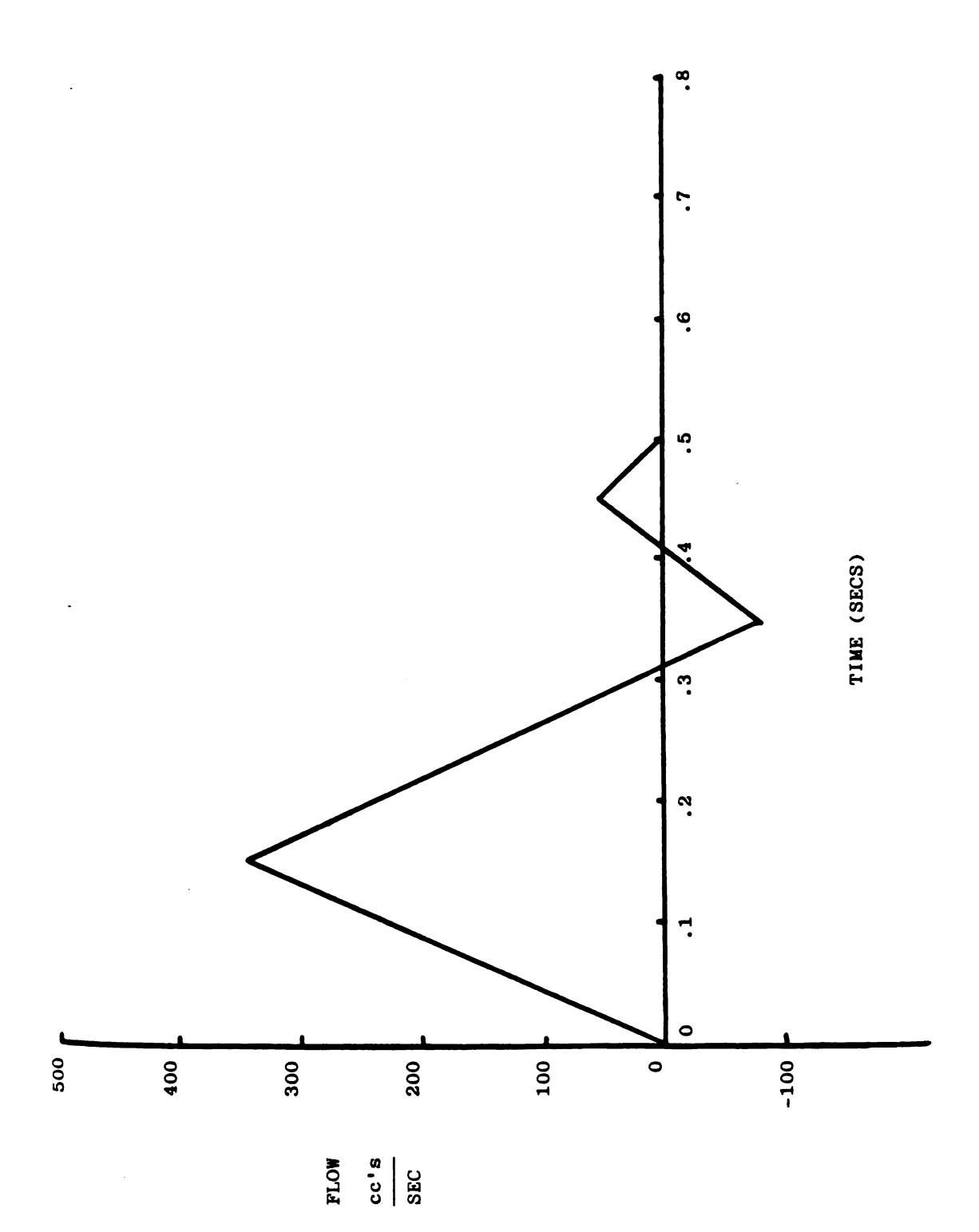


Figure 5.3
Aortic Flow in Penn State Arterial Model

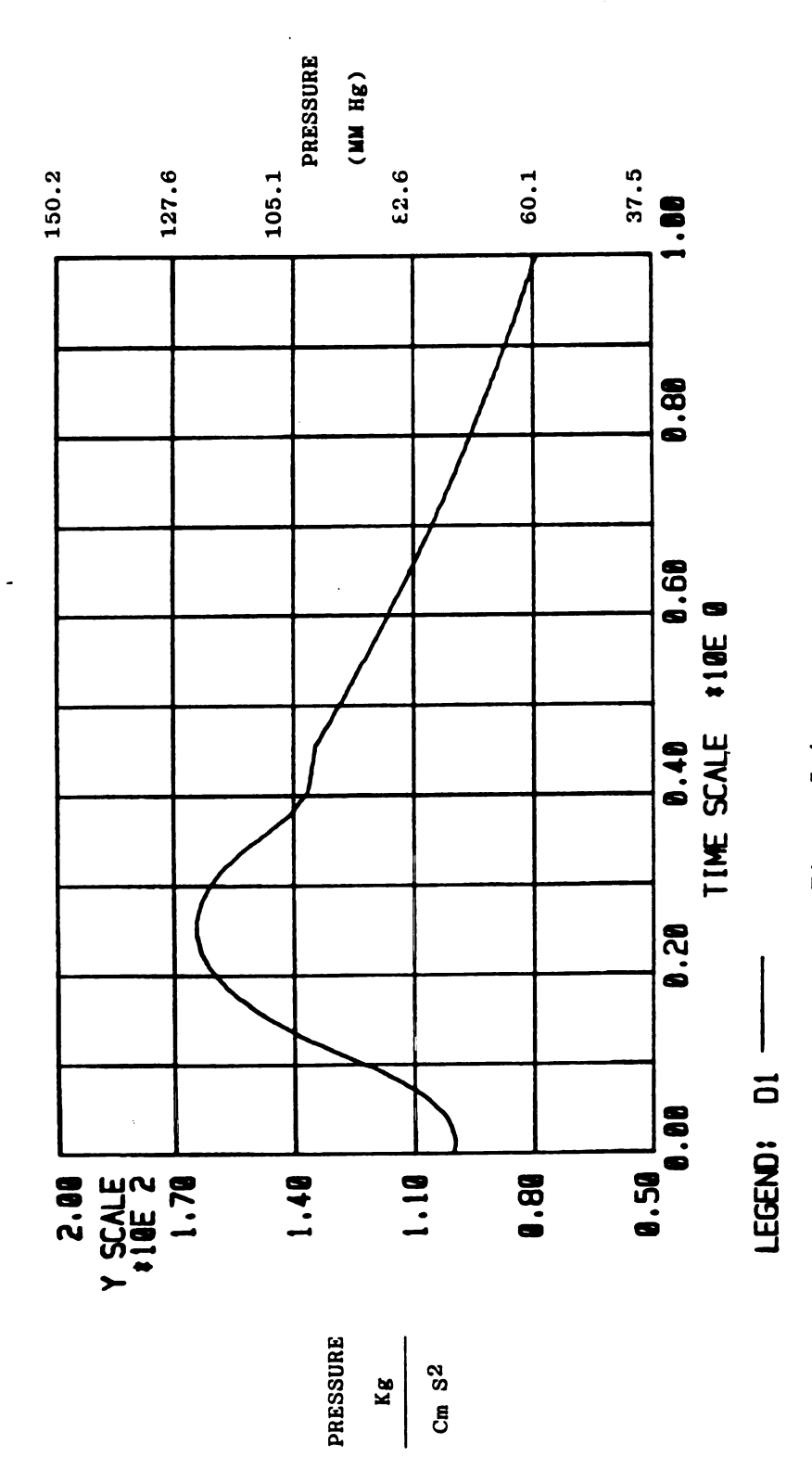


Figure 5.4 AORTIC PRESSURE FROM PENN STATE ARTERIAL MODEL

CHAPTER 6

EXPERIMENTAL RESULTS

STATIC COMPLIANCE

Static compliance values for various tubing materials and sizes are listed in Table 6.1.

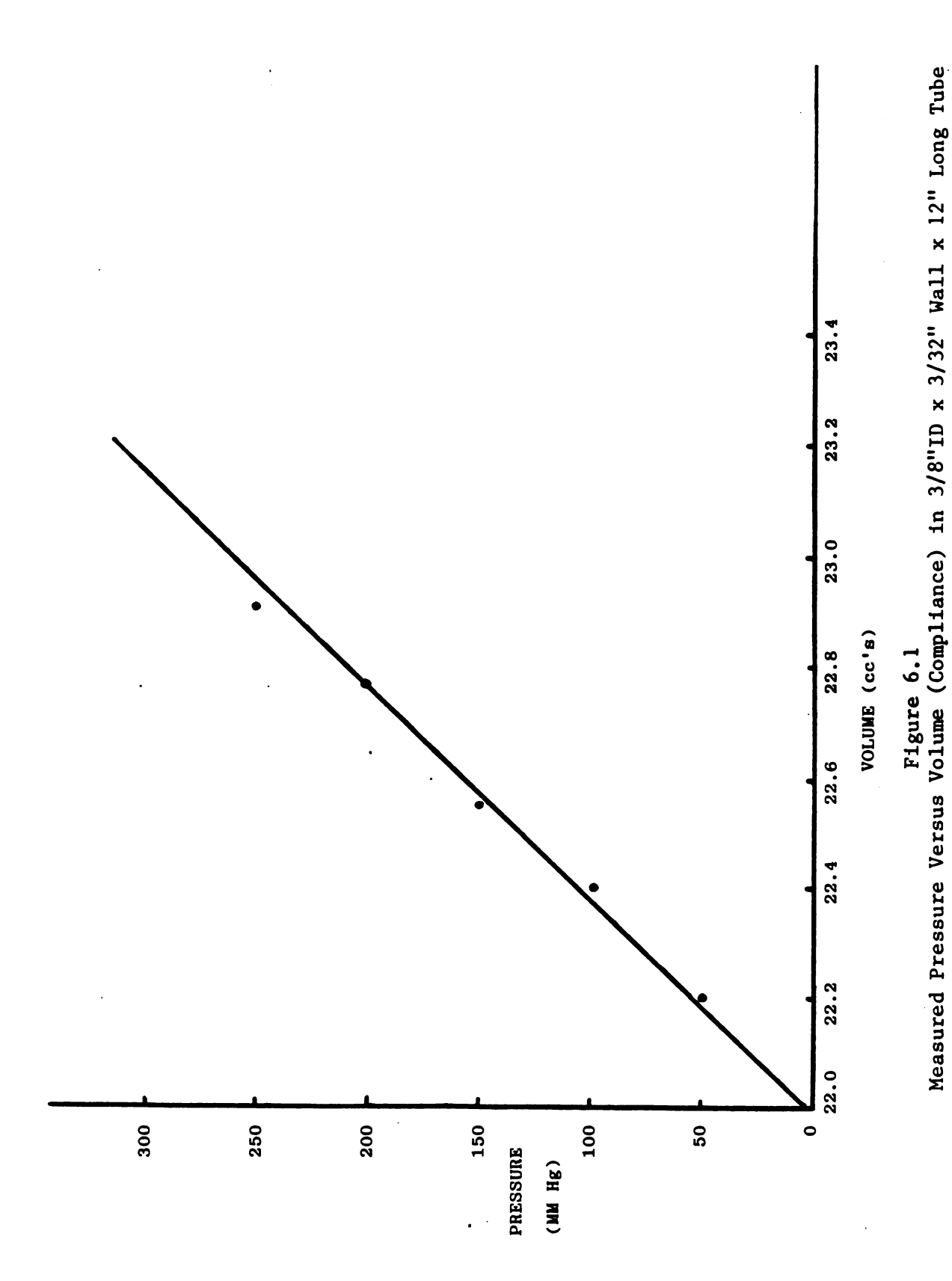
TABLE 6.1
Static Compliance Values (1 ft. length)

Material	ID	Wall	Compliance	
	inches	inches	cc/mmHg (cm ⁴ s ² /kg)	
PVC	3/8	3/32	0.0038 (0.0029)	
PVC	3/8	1/16	0.0048 (0.0036)	
Silicon	3/8	3/32	0.0045 (0.0034)	
PVC	1/2	1/8	0.0069 (0.0052)	
PVC	1/2	1/16	0.0084 (0.0063)	

Figure 6.1 plots the pressure as a function of the volume for 3/8" ID x 3/32" wall x 12" long (hereafter referred to as 3/8" x 3/32" x 12") PVC tubing. The slope is linear for the region between 0-300 mmHg but thereafter is nonlinear. Since most pressure will be assumed to be less than 300 mmHg during extracorporeal circulation, the linear compliance will be used.

Before the step input of pressure test was commenced, it was desired to predict the value of the wall resistance that would cause the system to be overdamped. Using the relation for critical damping developed in equation A.13, for 3/8" x 3/32" x 12" tubing:

$$\begin{pmatrix} R_3 + R_4 + R_9 \end{pmatrix}^2 = \frac{1}{I_2 C}$$



where the parameters have been previously defined to be:

$$R_3 = R_1 = 0.16 \text{ kg/cm}^4$$
 $R_4 = R_{ent.} = 0.0005 \text{ kg/cm}^4$
 $I_2 = 0.0428 \text{ kg/cm}^4$
 $C = 0.0029 \text{ cm}^4 \text{s}^2/\text{kg}$

for a one foot length of tubing. The system will be critically damped when the wall resistance, $R_{\rm q}$, is equal to:

$$R_q = 7.518 \text{ kg/cm}^4 / \text{unit length}$$

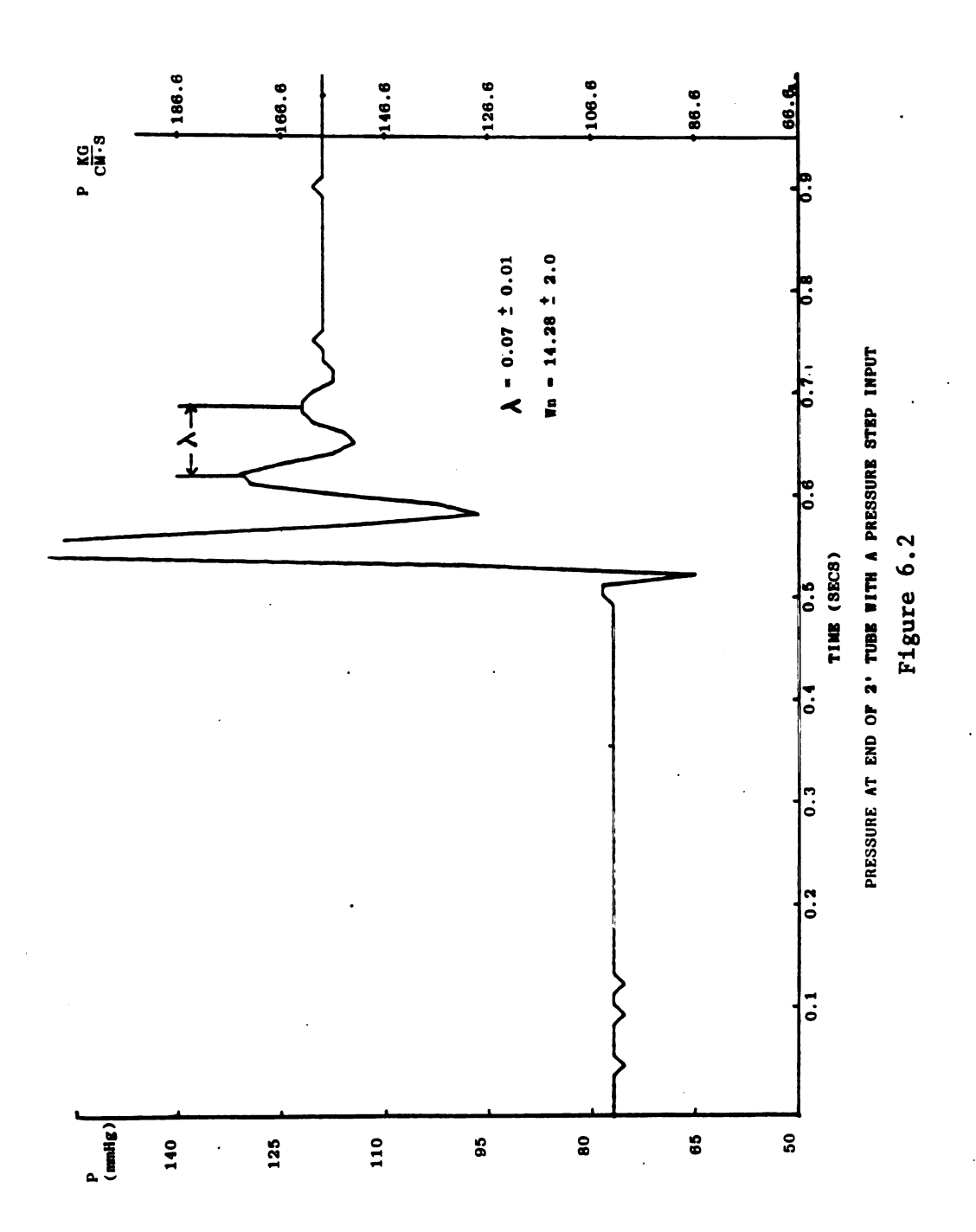
Since this value is very high, I would not expect the system to be critically or overdamped. Instead I would predict a vibration enclosed by a damping envelope. The natural frequency of this system is predicted by equation A.12 to be:

$$w_n = \sqrt{1/IC} = 89.7 \text{ rad/s or } 14.28 \text{ Hz.}$$

The actual step input test was performed on two feet of 3/8" x 3/32" PVC tubing so its predicted natural frequency would be:

$$w_n = \sqrt{1/(2Ix2C)} = 44.88 \text{ rad/s} = 7.14 \text{ Hz}.$$

Figure 6.2 shows the actual response of two feet of tubing subjected to a step pressure increase from approximately 80 mmHg (106.6 kg/cm s^2) to around 120 mmHg ($160.\text{kg/cm s}^2$). As expected the system is underdamped. The natural frequency is found by measuring the wavelength from peak to peak. The natural frequency in hertz, is the inverse of the wavelength. In this case the actual measured natural frequency is $14.28 \pm 2.4 \text{ Hz}$. The deviation represents the inaccuracy of measuring the wavelength. The percent error that the measured or actual frequency deviates from the predicted frequency is:



In this initial case there is a 50% error between predicted and actual frequencies. This is a sizeable error but is understandable considering the crudeness of a one element model. Table 6.2 shows the effect of increasing the number of elements on the predicted frequency and the error percentage.

TABLE 6.2

Effect of Number of Segments on Accuracy (2 Foot Tube)

# Segments	Predicted	Actual	% Error	
	Frequency	Frequency		
	Hz.	Hz.		
1	7.14	14.28 ± 2	50.	
2	9.9	14.28 ± 2	30.7	
4	11.13	14.28 ± 2	22.1	
8	11.77	14.28 ± 2	17.6	

DYNAMIC COMPLIANCE

It is apparent that the number of elements seems to be a prime factor in the ability of the model to accurately predict the behavior of the actual system. The last attempt with eight element is approaching an acceptable range since the actual frequency could be anywhere from 12.28 to 16.28 Hz. 12.28 Hz represents an error percentage of only 4.1% from the predicted response of 11.77 Hz. However, the system seems to be nearing an assymptotic value which will predict a lower frequency than the measured frequency of 14.28 Hz. It was assumed that the static compliance is actually higher than the dynamic compliance of the tubing wall during transient conditions. A lower dynamic compliance means the tubing was stiffer during a time varying load. Bergel found arteries

felt stiffer under dynamic loading so this concept of a dynamic compliance is not without precedent. The two segment, 2 foot tubing model was used to find a new dynamic compliance value which would predict a natural frequency of 14.3 Hz. Once this compliance was determined, it was tested in 3, 4, and 8 foot length models. The dynamic compliance for the two foot length was found to be:

$$C_d = 0.0013 \text{ cm}^4 \text{ s}^2/\text{kg/ft}$$

This dynamic compliance was used to predict the frequencies for the other lengths. The results are tabulated in Table 6.3.

TABLE 6.3 Predicted and Actual Frequencies with $C_{\rm dyn} = 0.0013~{\rm cm}^4 {\rm s}^2/{\rm kg/ft}$.

Length	Predicted	Actual		
	Frequency	Frequency		
ft.	Hz.	Hz.		
2	14.3	14.28 ± 2.		
3	10.3	10.0 ± 1.		
4	8.0	8.0 ± 0.6		
8	4.0	4.2 ± 0.2		

The deviation from the actual frequency diminishes because it becomes easier to measure the frequency with longer tube lengths and correspondingly, longer wavelengths. All the predicted frequencies fall within range of the actual frequency for that length.

WALL RESISTANCE

The compliance value under dynamic conditions could now be used with reasonable assurance. This value could be used to find the only

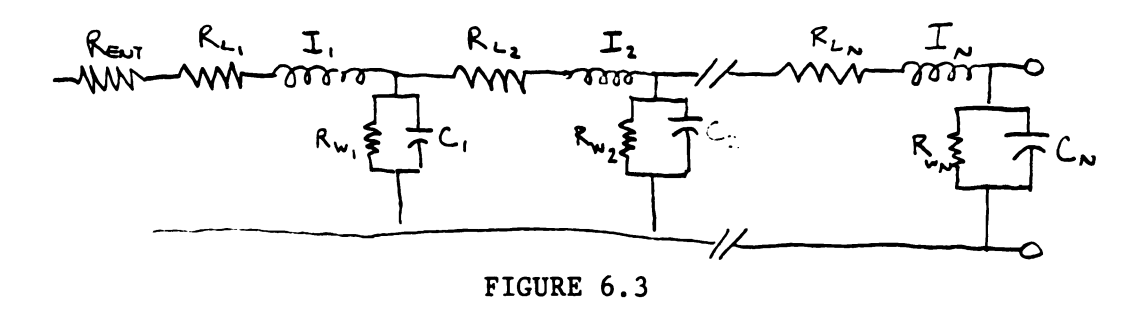
$$R_{tot} = R_1 + R_2 + \dots R_N$$

In the case of N parallel resistors the corresponding relation would be:

$$\frac{1}{R_{tot}} = \frac{1}{R_1} + \frac{1}{R_2} + \dots + \frac{1}{R_N}$$

R_{tot} in the parallel case must be less than any individual R value.

If the electrical analogue is extended to the tubing, several segments of tubing would be represented as shown in Figure 6.3.



N Segments of Tubing Represented by Electrical Analogue

The resistance resulting from entrance effects and those resulting from line friction would tend to add to a total resistance. However all the wall resistances would sum to a total wall resistance which is equal to or less than any of the individual elements since they are in parallel. Therefore, I concluded that either the entrance resistance or the value for each line resistance was in error. Since the line resistance had been determined empirically, whereas the entrance friction had been obtained from a handbook, I surmised that the latter was most probably in error. The problem now became trying to determine two unknown resistances (Rent and Rw) given only one equation. The solution was obtained through trial and error. Rent and Rw were found to fit the data for the two foot length and then these resistances were checked in models for longer lengths. The data was very difficult to fit because the damping envelope from the laboratory data, did not fit any type of linear model. I would like to briefly diverge onto the subject of determing whether a resistor is linear from the measured vibrational decay.

A convenient way to determine the amount of damping present in a simple single element system is to measure the rate of decay of the free vibrations. The solution to the state equation for the momentum flux of the fluid in a tube subjected to a step increase of pressure will be (the state equations were developed in Appendix A):

L = X exp(-E w_n t) sin ($1-E^2$ w_n t + z) EQN. 6.1 where X is an arbitrary constant, E is the ratio of the damping to the critical damping, and z is the phase angle between L and the forcing function. The effort or pressure is a more familiar quantity than the momentum flux and it is simply the derivative of this function for L or: $P = -X E w_n^2 (1-E^2) \exp(-E w_n t) \cos(1-E^2 w_n t+z) EQN. 6.2$

I would like to introduce a term called the logarithmic decrement which

is the natural logarithm of the ratio of ANY two successive pressure amplitudes as defined in equation 6.2. In linear theory this is an appropriate assumption if the ratio of all successive pressure amplitudes are equivalent. However, in the case of the free vibrations measured as a result of the step pressure input (see Figure 6.2), the ratio of the amplitudes are never close to being equal. Since these ratios were not equal, the system was not experiencing a linear resistance. Therefore, it would not be unusual to have difficulty fitting the data into a model comprised of linear resistances. My best fit for R_{ent} and R_w was:

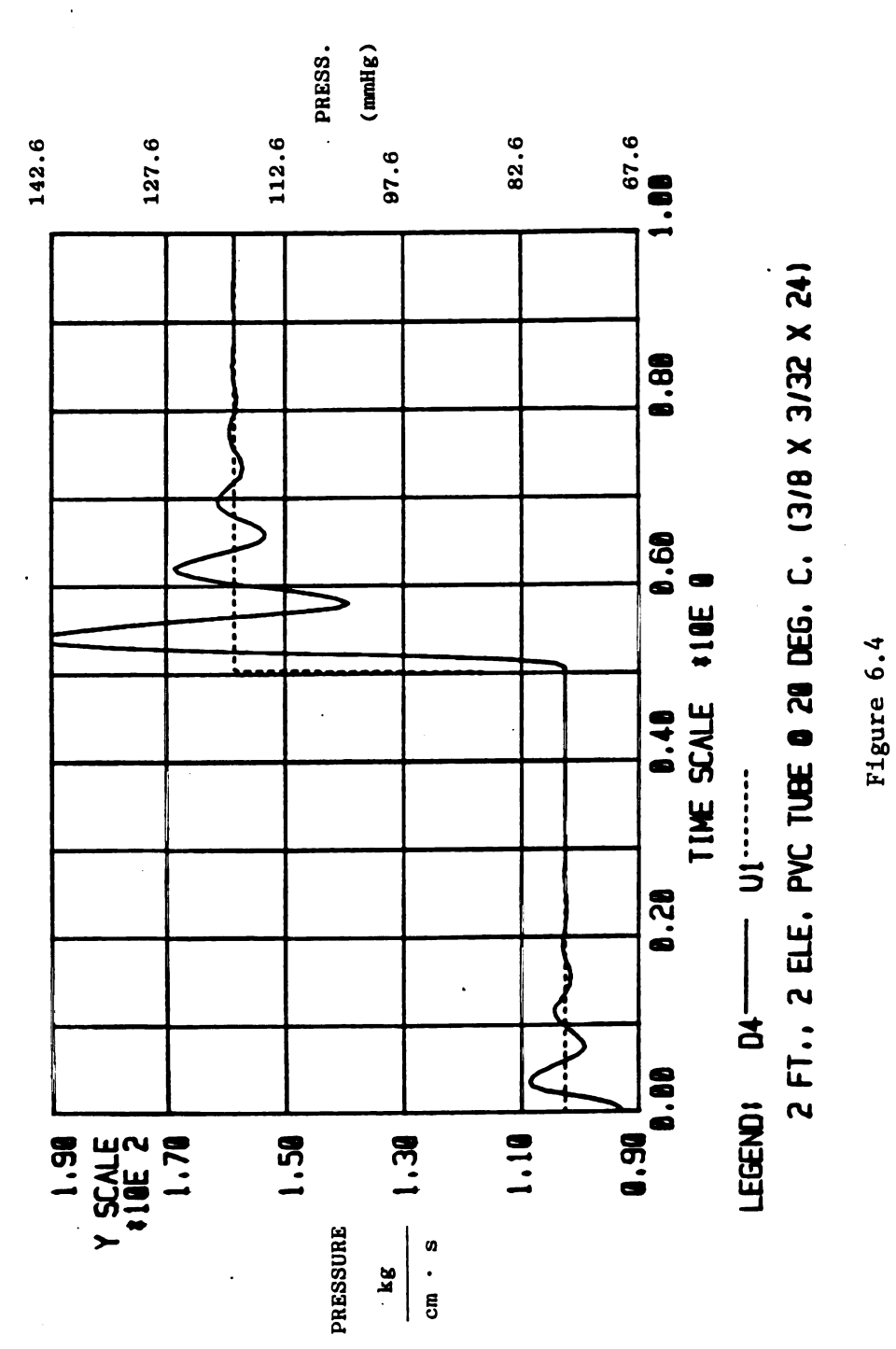
$$R_{ent} = 1. kg/cm^4$$

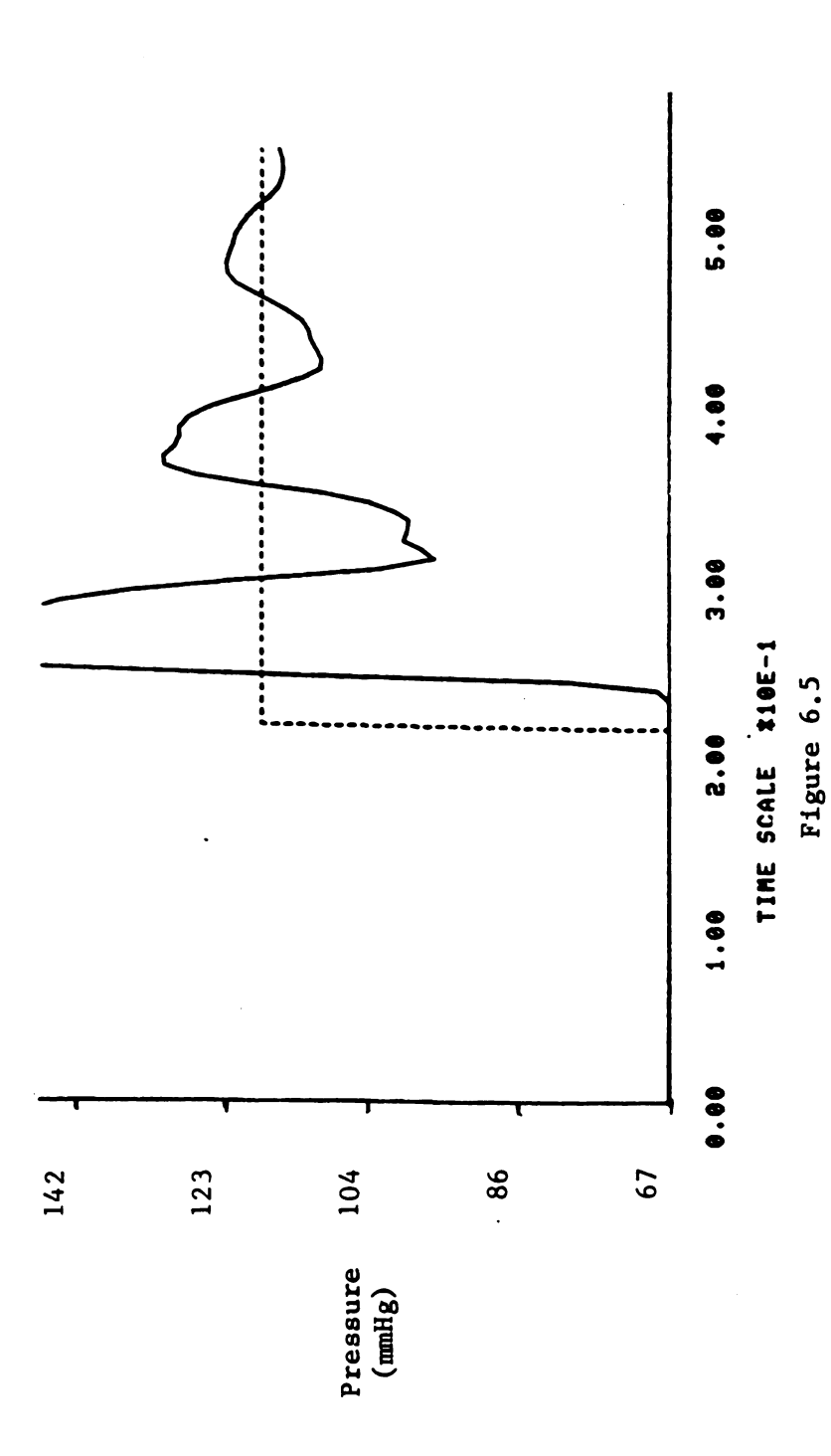
$$R_{ent} = 1.6 kg/cm^4/unit length$$

The computer simulation of this step input using the new resistance values is shown in Figure 6.4 for a two foot, two segment model and Figure 6.5 for a three foot, three segment model. The actual data obtained for two foot and three foot lengths are shown in Figures 6.2 and 6.6. The pressure amplitudes only roughly fit the data because of the inaccuracy of the linear resistance model.

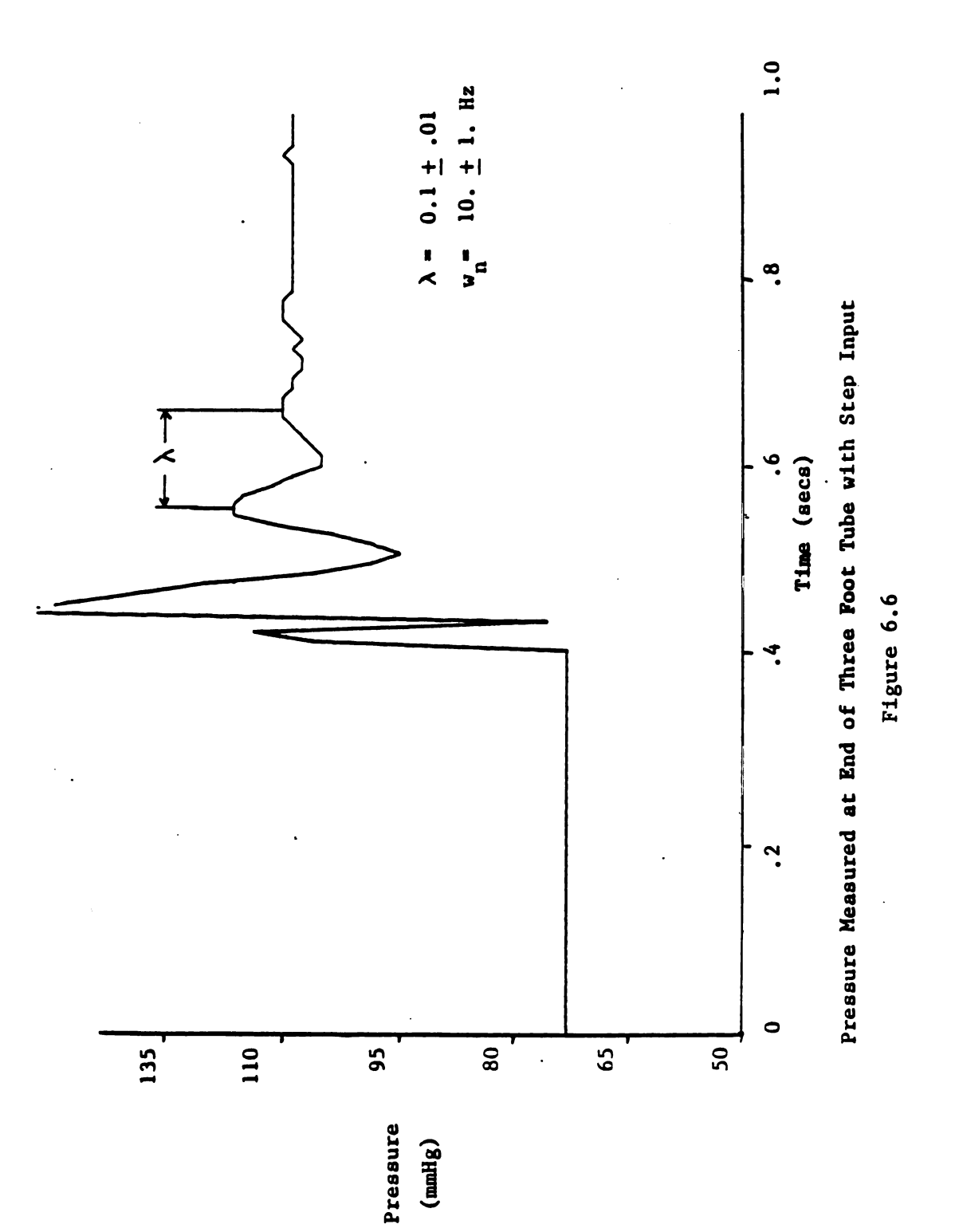
TEMPERATURE EFFECTS

The effects of temperature on the tubing characteristics were desired to be quantified. However, due to the lack of confidence in the model due to the supposition of linear resistance, these affects could only be shown qualitatively. The step input test was done under elevated temperatures for various tubing sizes and these empirical results permit an understanding of the general trends. The subtle changes in resistance caused by increased temperature were too sensitive to be measured with the computer model.





Predicted Pressure in a Three Foot Tube



The procedure for changing temperature was to initially fill the reservoir with approximately 40°C water. The tubing specimens were connected and quickly filled with water at approximately 37°C. The system was pressurized and the test run very rapidly to prevent a temperature drop of any significance. The measured and predicted frequency response along with the value for the dynamic compliance for each case are tabulated in Table 6.4.

There was little measurable change in the measured natural frequency of the tubing with increased temperature. Since the density of the fluid would not change significantly and therefore the inertia would remain constant, I conclude that temperature does not significantly affect the compliance of the tubing. The natural frequencies, predicted and actual, with dynamic compliance values for various tubing sizes are also included in the table. Wall thickness does not seem to affect the dynamic compliance significantly.

TABLE 6.4

Natural Frequency and Dynamic Compliance as a

Function of Tube Size and Temperature

ID	Wall	Length	Temp.	w _n	w _n	C _{dyn}
				Pred.	Actual	
in.	in.	in.	°C	Hz.	Hz.	$cm^4s^2/kg/ft$.
3/8	3/32	24	20	14.3	14.28 ± 2	2.0 0.0013
3/8	3/32	24	37	14.3	14.28	0.0013
3/8	3/32	36	20	10.3	10.0 ± 1	0.0013
3/8	3/32	36	37	10.3	10.0	0.0013
3/8	1/16	24	20	14.3	14.28 ± 2	2.0 0.0013
3/8	1/16	24	37	14.3	14.28	0.0013
1/2	3/32	36	20	6.8	7.14 ±	.6 0.0025

Temperature does seem to affect the overall damping of the system. Upon examination of Figures 6.2 and 6.7, it is apparent that temperature increase causes a decrease in the wall resistance. This cannot be quantified due to the limitations of the tubing model previously mentioned.

PULSATILE INPUT EXPERIMENT

The third experiment involved introducing a pulsatile flow to the tubing, the parameters of which were fairly well estimated. Downstream of the tubing was a resistor (ball valve) with variable degrees of occlusion which was fixed for all these tests. The value of the resistance was found by measuring the pressure drop across the resistor

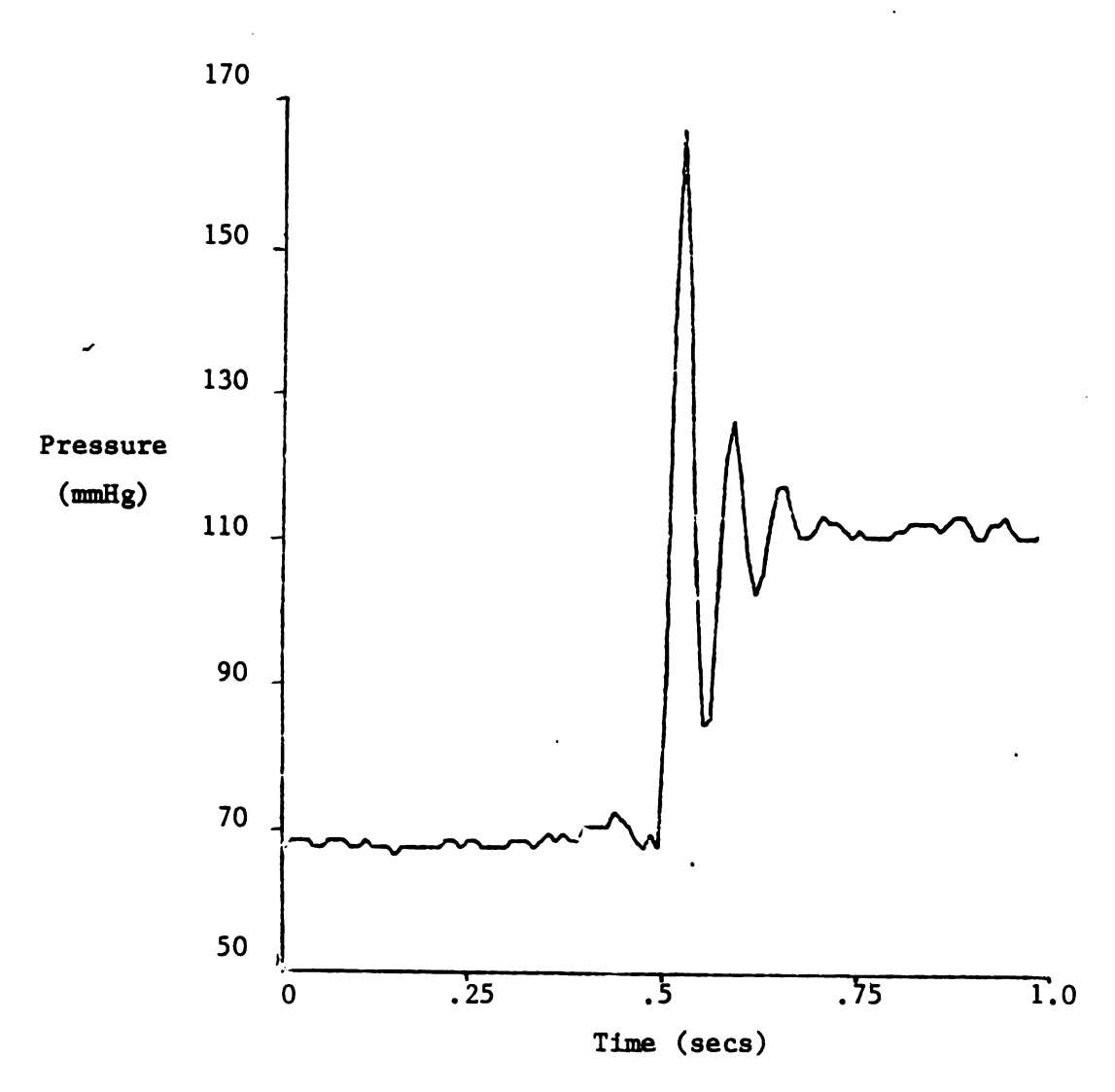


Figure 6.7

Measured Pressure in 2' Tube with Step Input (37° C.)

while simultaneously measuring the flow rate. The values for the upstream pressure (P_1) , downstream pressure (P_2) , and the flow rate (Q) were:

$$P_1 = 75 \text{ mmHg}$$

$$P_2 = 55 \text{ mmHg}$$

$$Q = 50 \text{ cm}^3/\text{s}$$

The value of the resistor is then:

$$R = (P_1 - P_2)/Q = 20 \text{ mmHg}(1.332 \text{ mmHg}) /50 \text{ cm/s}$$

$$R = 0.484 \text{ kg/cm}^4 \text{s}^2$$

A half inch I.D. header which was approximately eight inches long extended from the point where the roller stopped to the 1/2" to 3/8" connector. Two and eight foot lengths of tubing were inserted between the connector and the ball valve. The pump was pulsed at one, three, and six liters per minute with no baseline flow and a pulse rate of 60 bpm with no discernable change in the vibrational characteristics of the tubing. This led me to conclude that the load rate did not significantly affect the compliance of the tubing: an important conclusion if the previous compliance values could be used generally. The bond graph for a two foot, two segment model with header, and a resistor at the end is shown in Figure 6.8. The parameters for this model were:

Header:
$$I_6 = 0.016 \text{ kg/cm}^4$$

 $1/2" \times 3/32" \times 8"$ $C_5 = 0.0036 \text{ kg/cm}^4$
 $R_4 = 1.0 \text{ (wall resistance)}$
 $R_7 = 0.078 \text{ kg/cm}^4 \text{s}^2$

Tubing:
$$I_{13} = I_{20} = 0.0428 \text{ kg/cm}^4$$

 $3/8$ " x $3/32$ " x 24 " $C_{12} = C_{19} = 0.0013 \text{ cm}^4 \text{s}^2/\text{kg}$
 $R_{11} = R_{18} = 1.6 \text{ kg/cm}^4$
 $R_{14} = R_{21} = 0.16 \text{ kg/cm}^4$

Valve: $R_{25} = 1.5$ (includes valve and exit effects)

Pressure Tap $I_{23} = 1$. (arbitrary value)

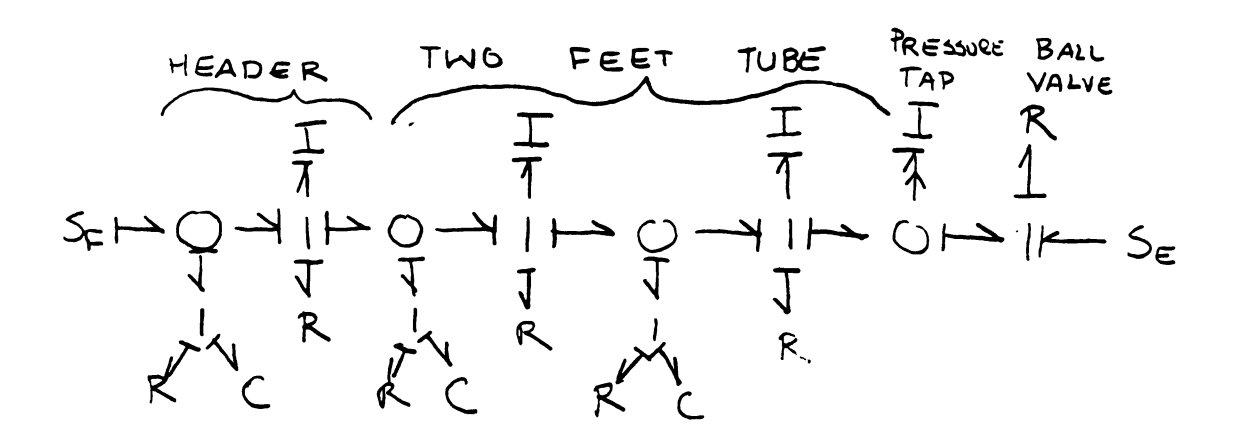


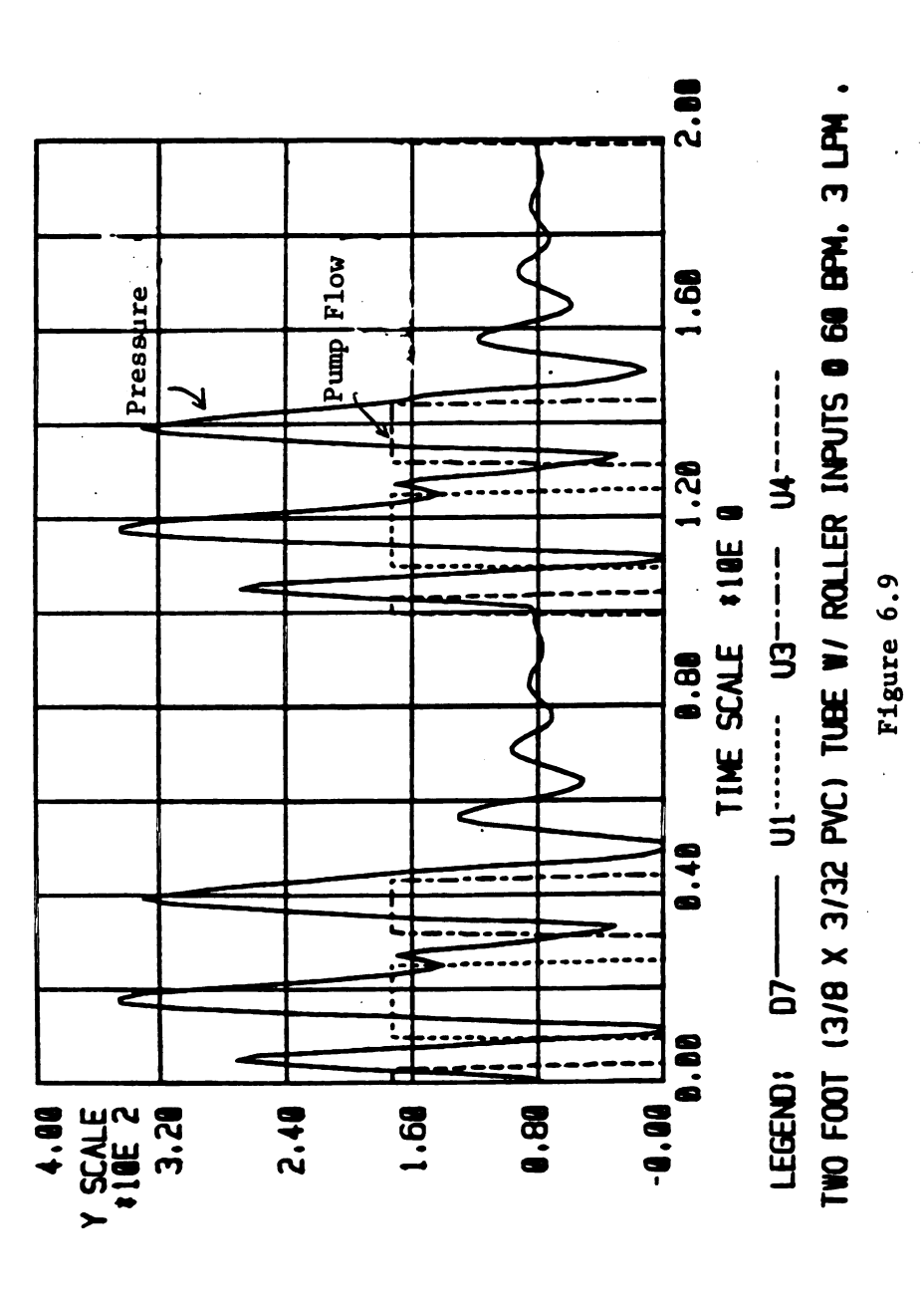
FIGURE 6.8

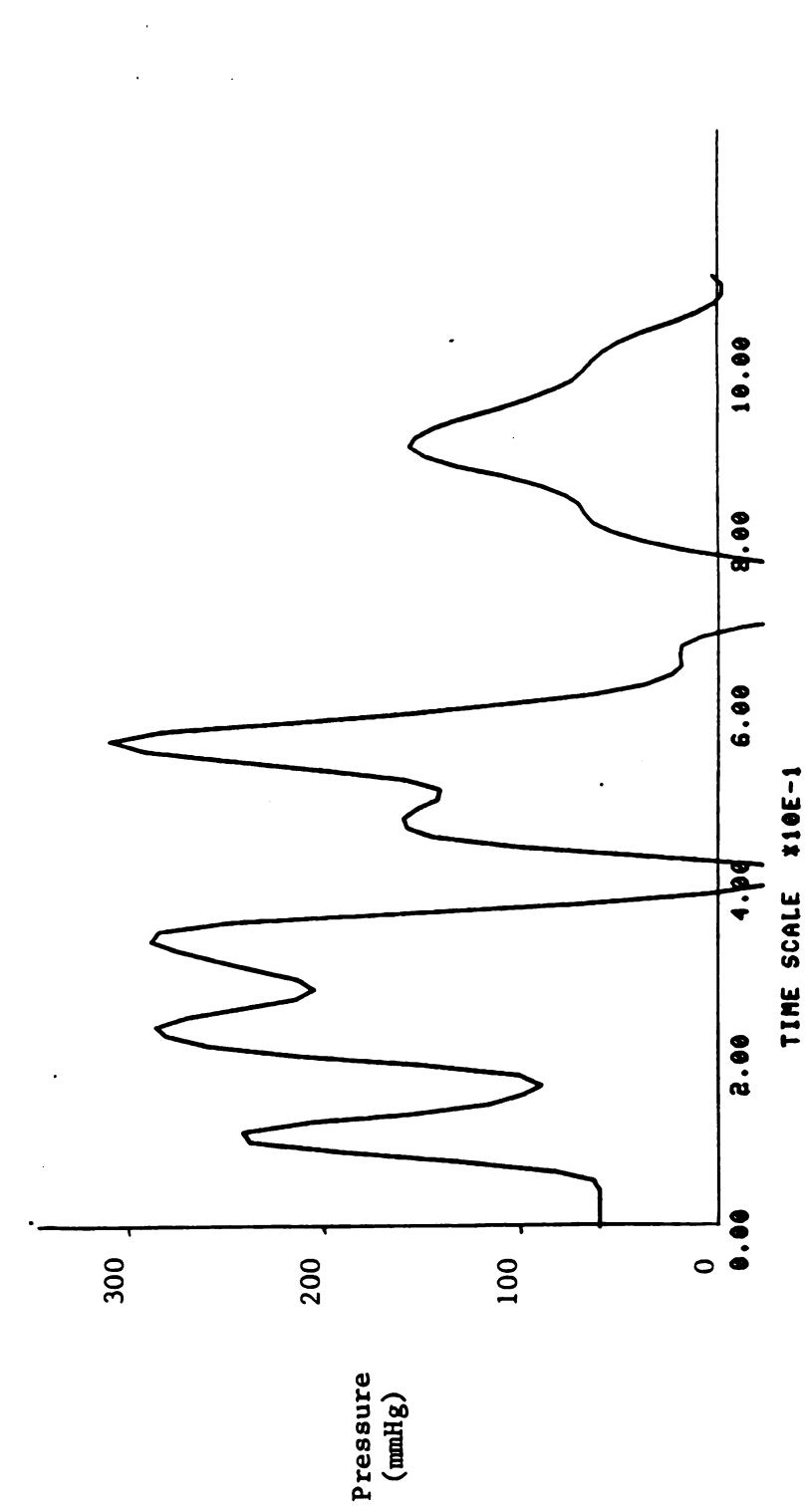
Bond Graph for the Pulsatile Tubing Test

The computer model for this system predicted the pressure response at the activated bond (pressure tap) as shown in Figure 6.9. The solid line represents the pressure read at the pressure tap while the dotted line is the flow input. As previously discussed, this model is only an approximation since tubing characteristics vary continuously with the position of the roller on the header tube. The exit resistance could only be estimated. Thus many parameters influencing this system were only estimated. The model was extended to predict the response of the identical system with eight feet of tubing. The computer simulation of the pressure at the pressure tap is shown in Figure 6.10. The actual measured pressures over a two second interval are shown in Figures 6.11 and 6.12 for the two and eight foot lengths respectively. The inability to firmly evaluate all the parameters detracts from the models accuracy. It was considered pointless however, to struggle improving the model since it can only be applied to the extremely limited case of 60 bpm, 3 lmp. At other flow rates and pulse rates the roller will not stop at the same place with every cycle and therefore parameters would be continuously changing. The decision was made to live with the inaccuracies of the model since the primary interests were the trends induced by changing parameters. Another drawback with religiously pursuing the accuracy of this model was that the arterial model was a very gross approximation of the human arterial system. Any precision gained in one model would simply be washed out in the imperfections of the other model. However, the qualitative effects of changing parameters could presumably be observed with this model.

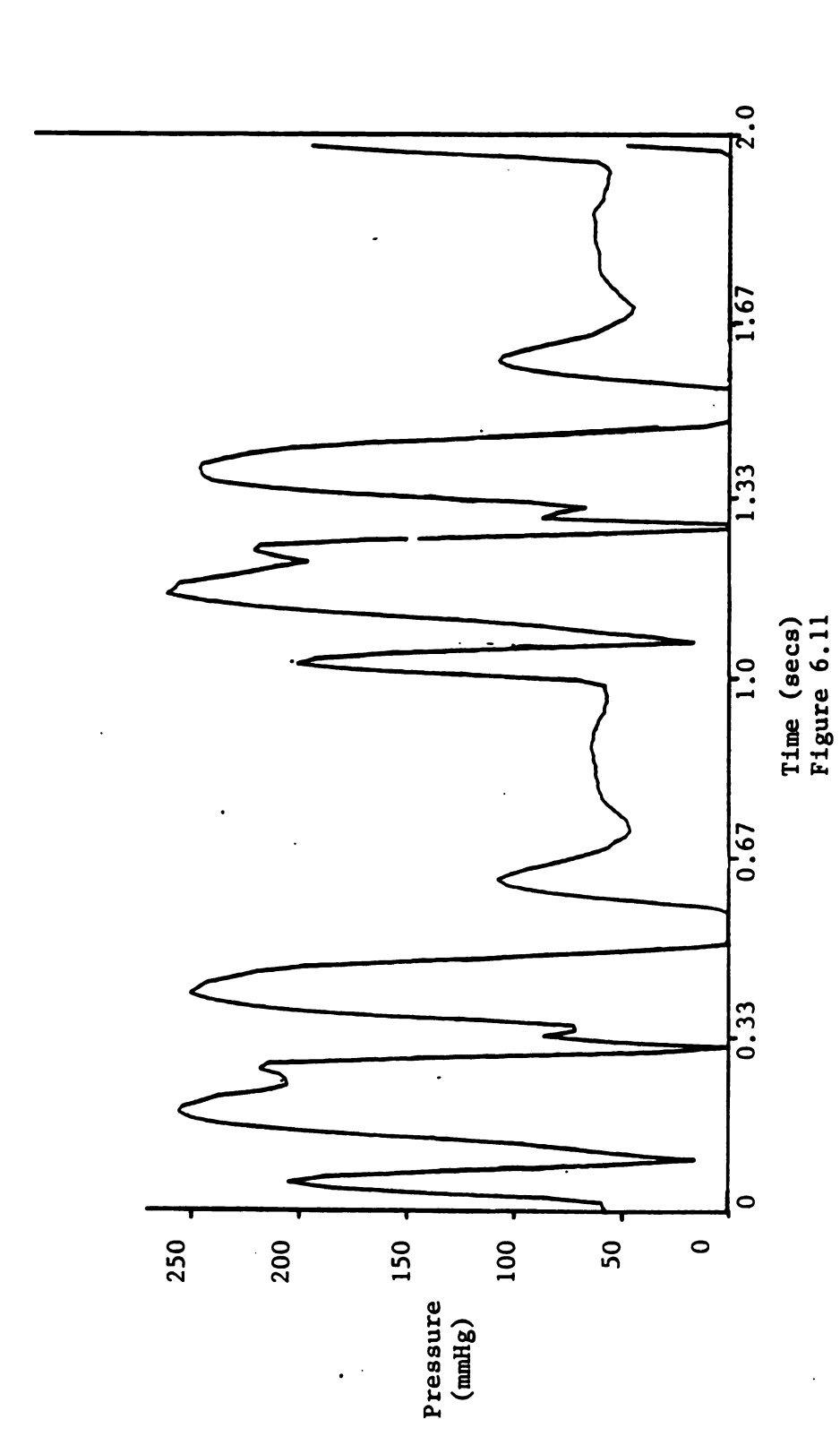
EXTRACORPOREAL CIRCUIT MODEL

The computer model of the tubing with a pulsatile input and a ball valve resistance could now be combined with the arterial system model

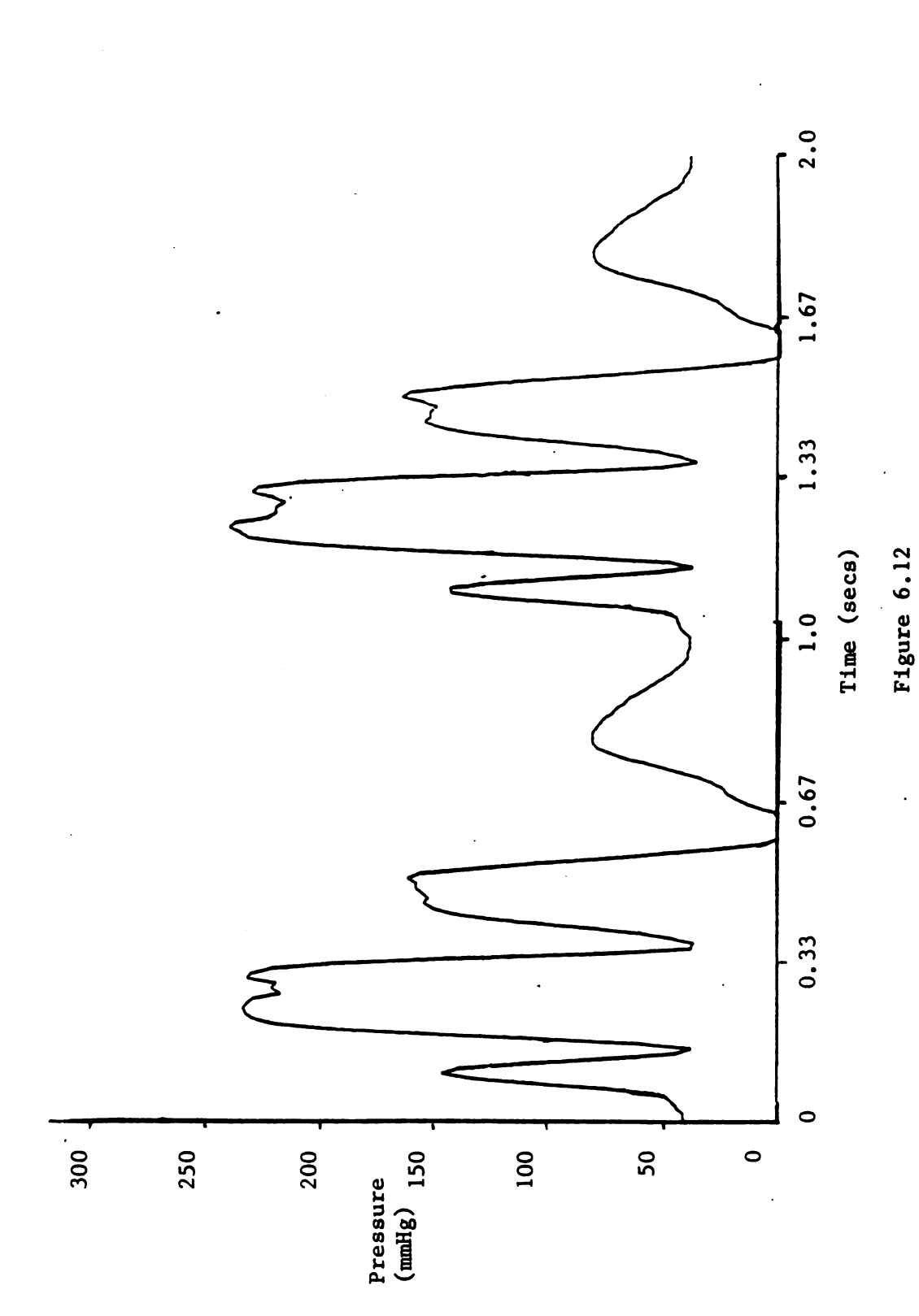




Predicted Response of Eight Feet of Tubing to Pulsatile Input (60 BPM, 3 lpm) Figure 6.10



Measured Pressure at End of Two Foot Tube With Pulsatile Input (60 Bpm, 3 Lpm)



Pressure Measured at End of Eight Foot Tube With Pulsatile Flow Input (60 BPM, 3 1pm)

circuit. The ball valve resistor was replaced with a cannula which was similarly modelled as a linear resistor. The resistance of the cannula was estimated from the relation of cannula flow rate to the pressure drop across the cannula in a study by Lynn Pfaender. The resistance was linearized and determined to be 1.2 kg/cm⁴ with a Sarns 8.0 High Flow cannula. A spring loaded accumulator was also included in this model for fine tuning. This accumulator was desired to filter out the high frequency pressure fluctuations arising from roller effects. The accumulator was simply modelled as a compliance C, which was initially set to a very low value of 0.001 cm⁴ s²/kg to negate its affects.

The bond graph and component diagram for this system is shown in Figure 6.13. An activated compliance element at the cannula will be used to predict the flow rate across the cannula while the two activated I elements predict the pressure just upstream of the cannula and also in the aorta. This model can be expanded to include various tubing lengths simply by changing the number of segments. The aortic pressure Predicted by the model is shown in Figure 6.14. Parameters for the tubing and header are the same as those listed on pages 46 and 47 and those for the arterial system are listed in Table 5.1.

EFFECT OF CHANGING TUBING LENGTH

The complete model could now be used to evaluate the effect on the blood flow dynamics from changing some of the extracorporeal parameters. Tubing length is of course of great interest since the length of tubing used in surgery will vary considerably from one operating theatre to the next. Figure 6. 15 shows the aortic pressure with a pulsatile flow input with various tubing lengths. All conditions were held constant

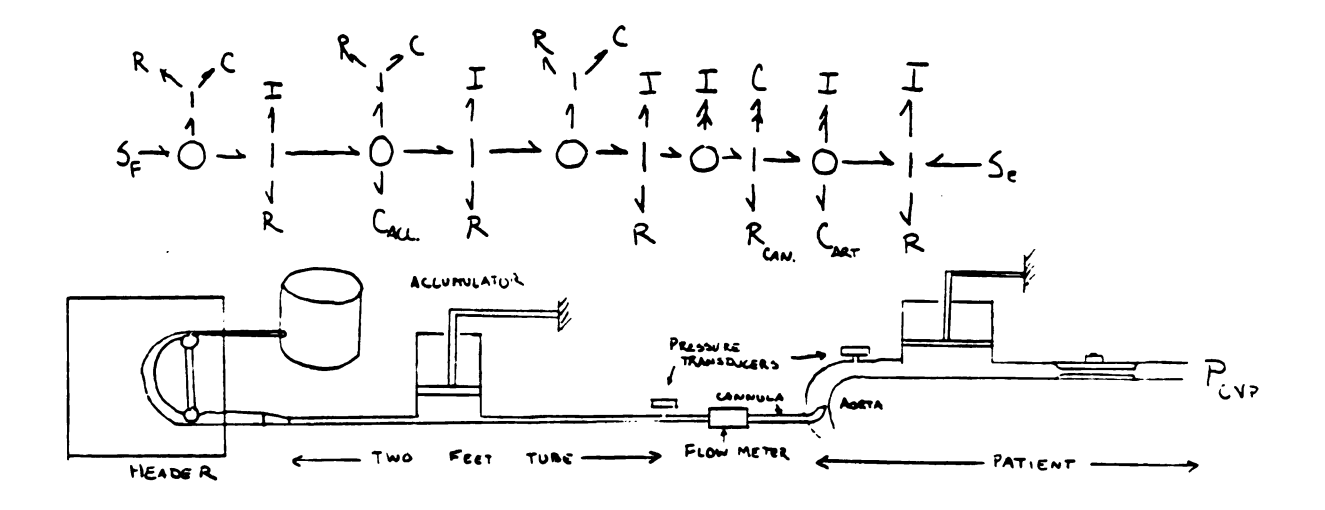
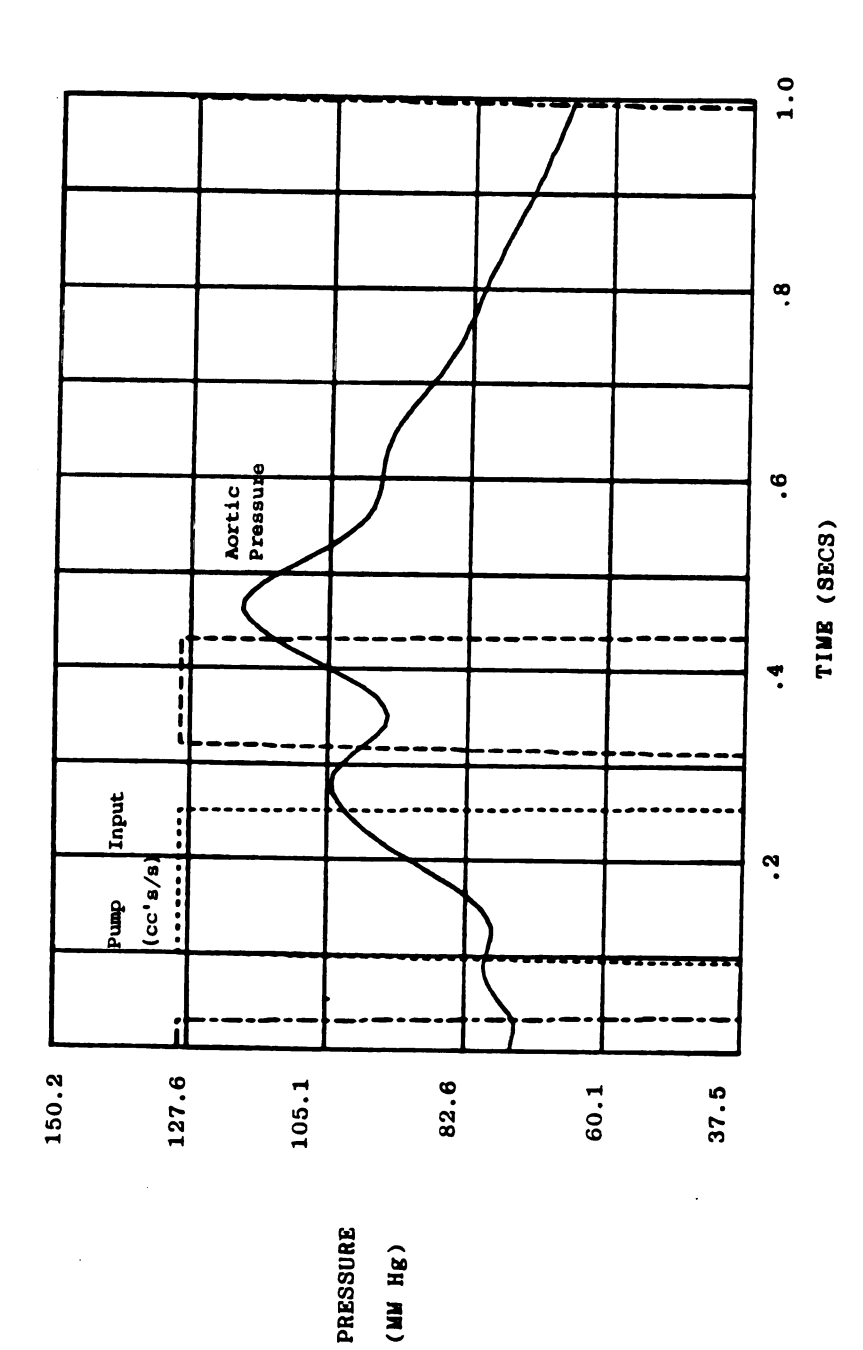


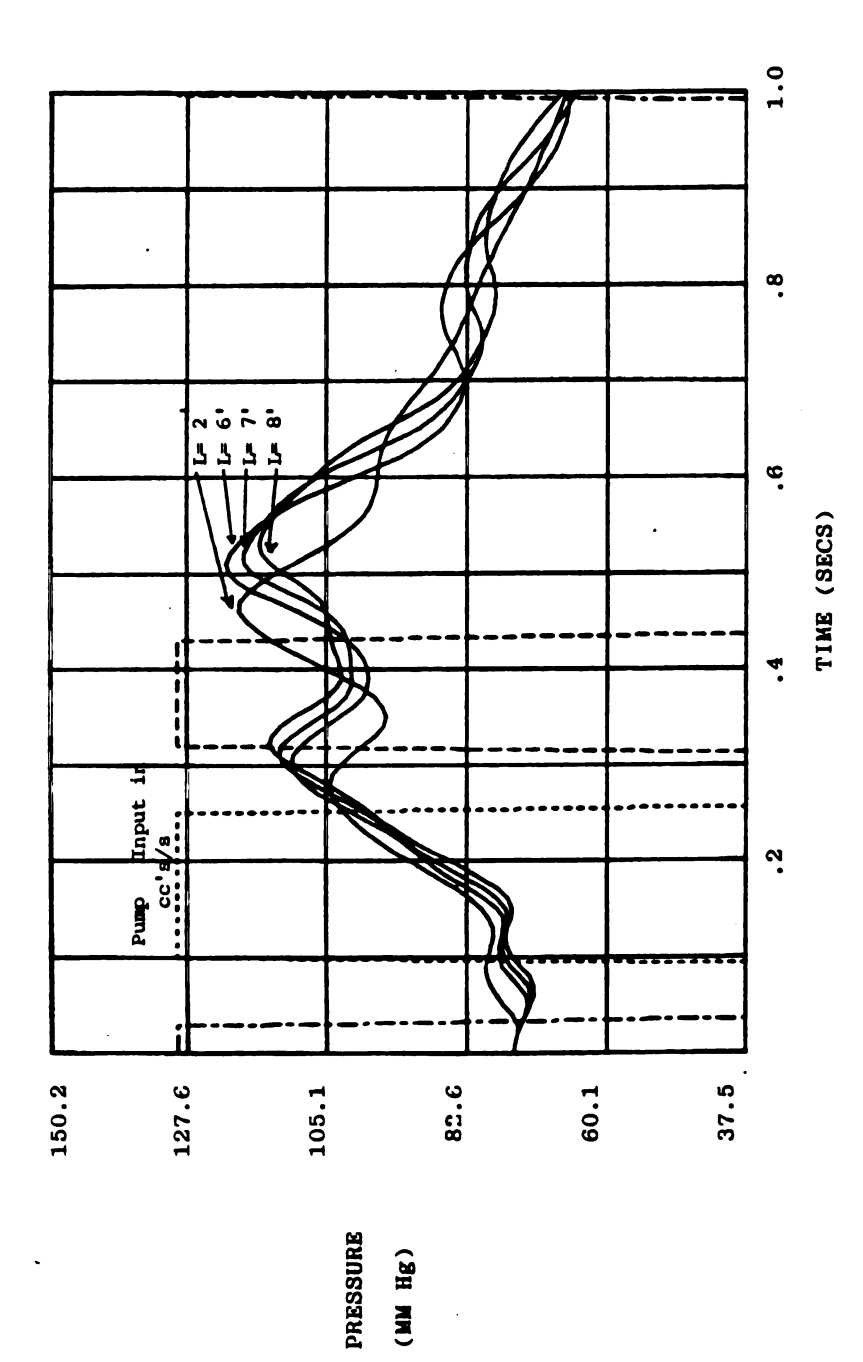
Figure 6.13

Bond Graph and Component Diagram for Two Foot Tube with Mock Arterial System



AORTIC PRESSURE WITH TWO POOT TUBE AND ROLLER INPUT

Figure 6.14

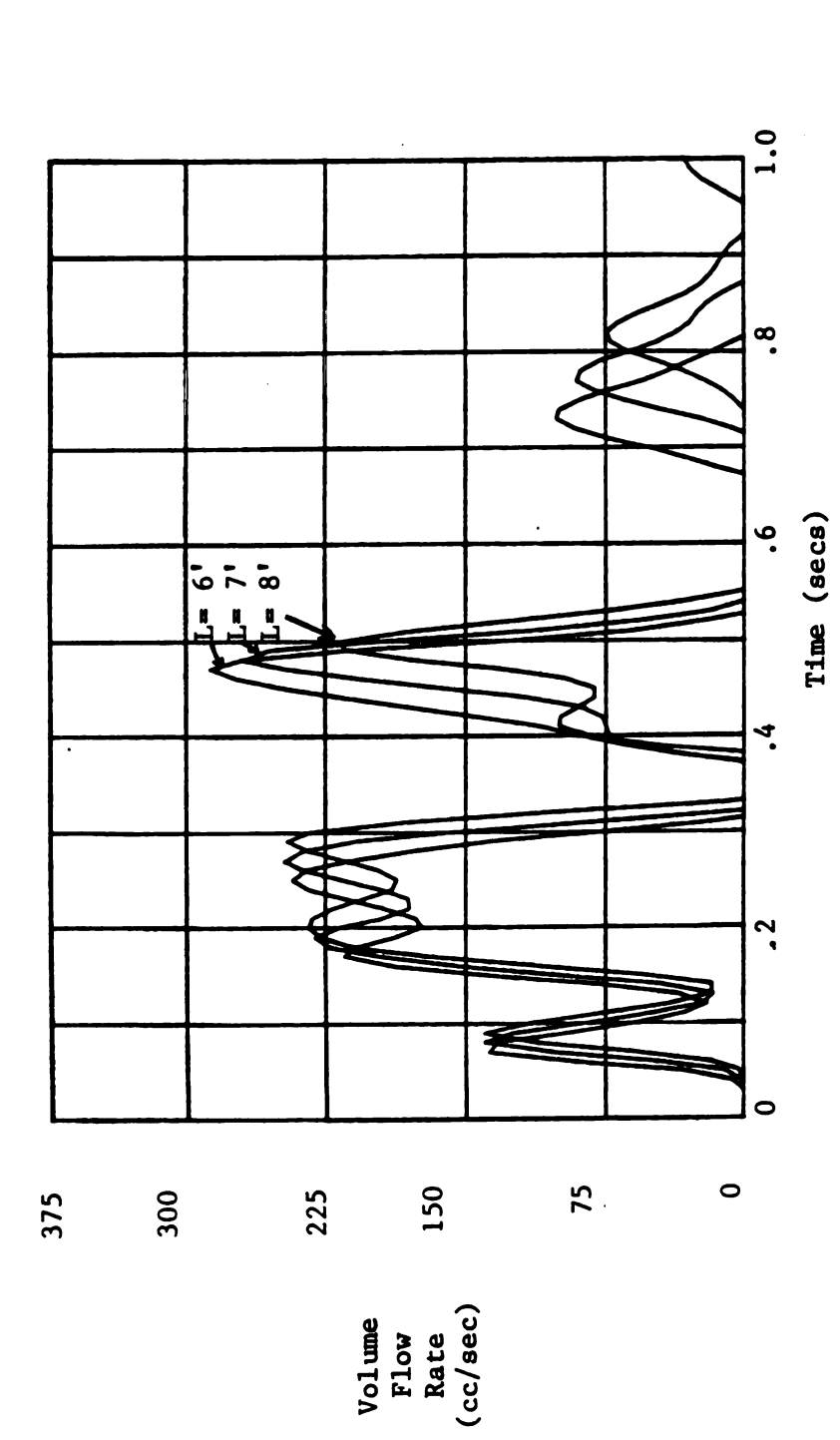


EFFECT OF TUBING LENGTH ON AORTIC PRESSURE

F1gure 6.15

except for the number of segments used in the model. In general it can be seen that tubing length does not significantly alter the aortic pressure wave. The longer lengths are slightly more damped due to the increased viscous and wall friction and the pressure fluctuation magnitudes are less severe owing to the fact that the longer tubes are more compliant. One of the most important parameters however is the rising pressure slope of the wave. Several researchers have commented on how the baroreceptors appear to be sensitive to rate of pressure change with time. Tubing length does not appear to influence this key parameter very much. The arterial pressure from the modelled Penn State mock arterial system shown in Figure 5.4 has a pressure rise of about 125-175 mmHg in 0.2 seconds. Therefore, the rising slope is approximately 250 mmHg/sec. This is certainly within range of a typical non-hypertensive patient. The rising slope of an eight foot tubing length with flow coming from a pulsatile pump is about (115-175/0.15 secs) or 266.7 mmHg/sec. Thus, there is little difference between the rising slopes of the normal arterial pressure wave and the wave coming from an assist pump with eight feet of tubing. This is an important result since it would seem to indicate that the patient's baroreceptors should not be sensitive to the difference between natural and assisted perfusion with regard to the slope of the rising pressure wave.

The flow rate through the cannula with varying tube lengths is shown in Figure 6.16. This indicates that again there is not a substantial change in flow rates with changing tubing length but the velocity fluctuations are slightly less severe and more damped with longer tubes. An interesting fact that can be observed from Figure 6.16 is that there is negative flow through the cannula which is not a



Effect of Tube Length on Volume Flow Rate Through the Cannula

Figure 6.16

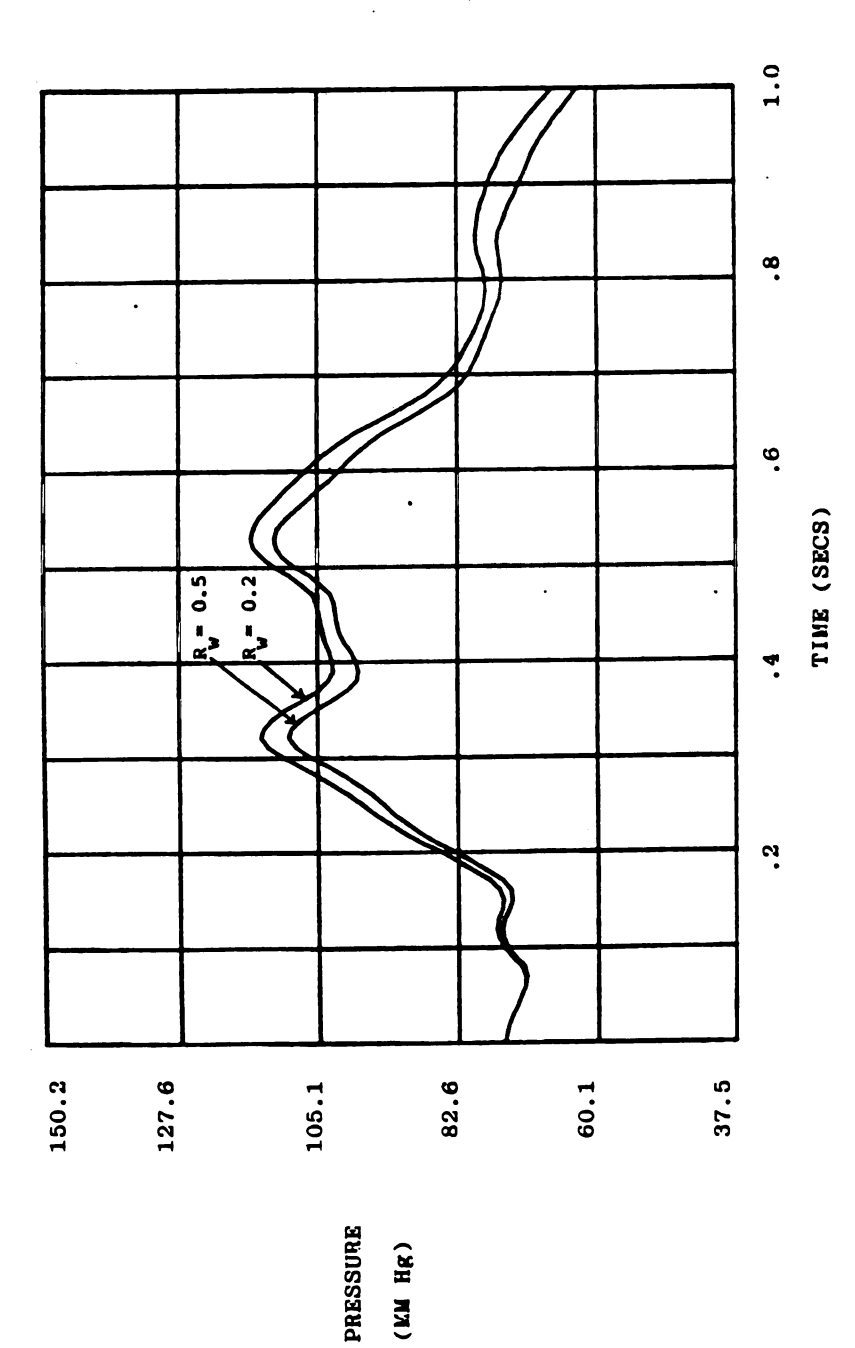
favorable condition. Much hemolysis (damage to red blood cells) can be attributed to backflow through the cannula since the transition from cannula to aorta is very abrupt and, therefore, highly resistive. It might be of use to include a check valve in future cannula designs to prevent backflow.

EFFECT OF CHANGING TUBING WALL RESISTANCE

As discussed previously, higher fluid temperatures and thinner walled tubing both result in less wall resistance with little discernable change in the compliance of the tubing. This implies that at the start or finish of the operation when the patient's temperature is around 37°C the tubing wall resistance will be lower. This is rather intuitive since tubing feels softer at higher temperatures or with thinner walls. The aspect which may not be intuitive is the fact that the compliance of the tubing remains constant but this again results from the viscoelastic effects. The effect of lower resistance on aortic pressure is shown in Figure 6.17. The aortic pressure is less damped with smaller resistance. This result is not unexpected since less energy will be dissipated with lower resistances and therefore more energy will be available in the aorta. The resistance of 0.5 kg/cm^4 is the control resistance which was determined at room temperature (20°C). The lower resistance of 0.2 kg/cm was an estimated value of lowered tubing resistance. Again there is not a substantial difference between the two aortic pulse waves indicating that temperature or wall thickness changes will not result in radical wave attenuation.

EFFECT OF CHANGING CANNULA RESISTANCE

The value of the cannula resistance was found from linearizing the pressure drop versus flow rate curve of a Sarns 8.0 cannula. Since it



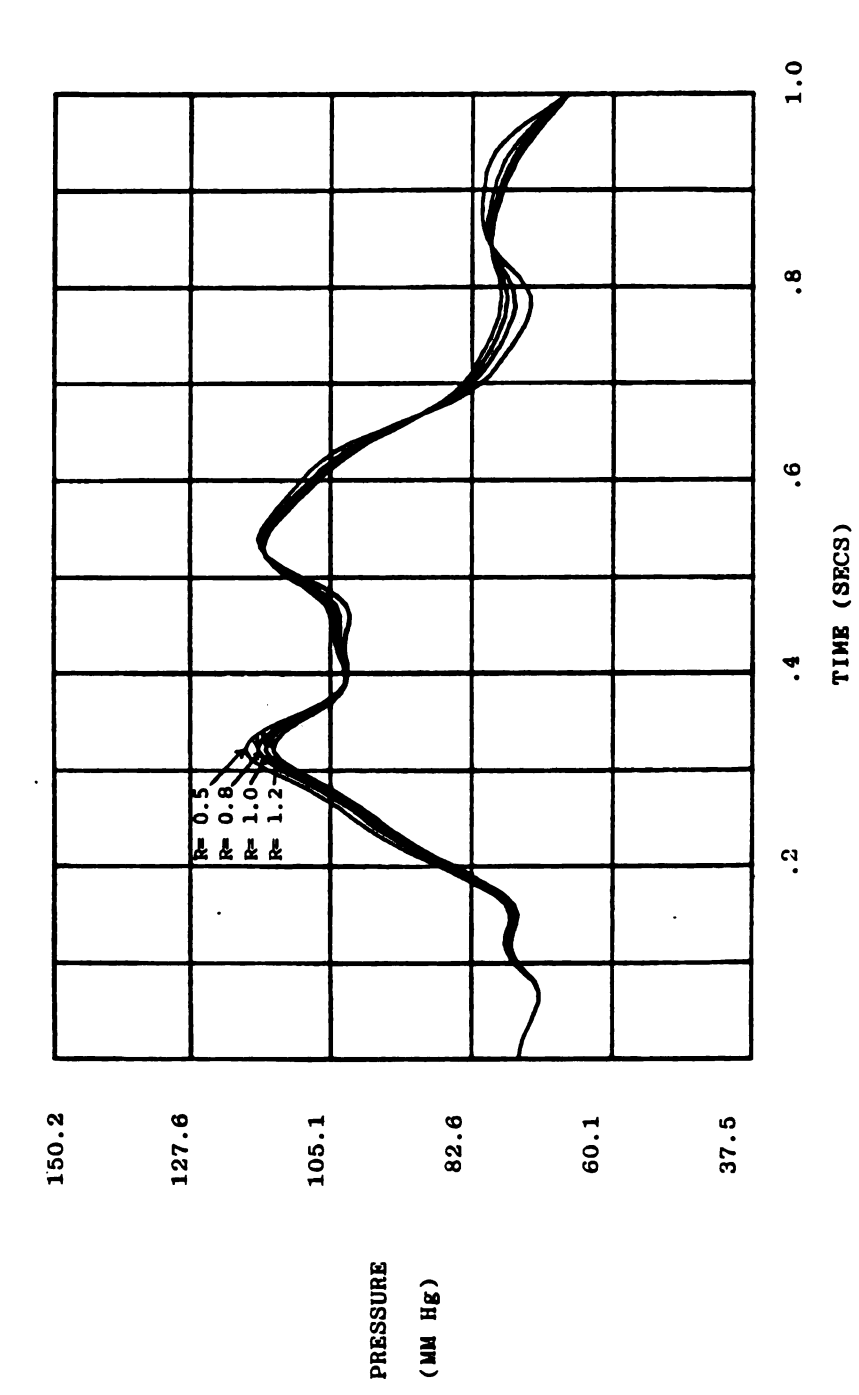
EFFECT OF TUDE WALL RESISTANCE ON AORTIC PRESSURE

Figure 6.17

was determined that entrance resistance effects appear to be fairly significant, it was of interest to see what the effect of lowering the resistance to flow would be on the dynamics of the circuit. Therefore the aortic pressure with a resistance of 1.2 kg/cm⁴ was plotted along with aortic pressures predicted from cannulae with diminishing resistance. This relation is shown in Figure 6.18. There is almost no difference between the various resistance values. The pressures predicted just upstream of the entrance to the cannula are plotted in Figure 6.19 and these show much more profound effects due to cannula resistance changes. High cannula resistance does not seriously alter the aortic pressure but does cause much higher pressures in the tubing. Thus, the higher resistances seem to cause a log jam effect where the pressure is relatively constant downstream but is elevated upstream.

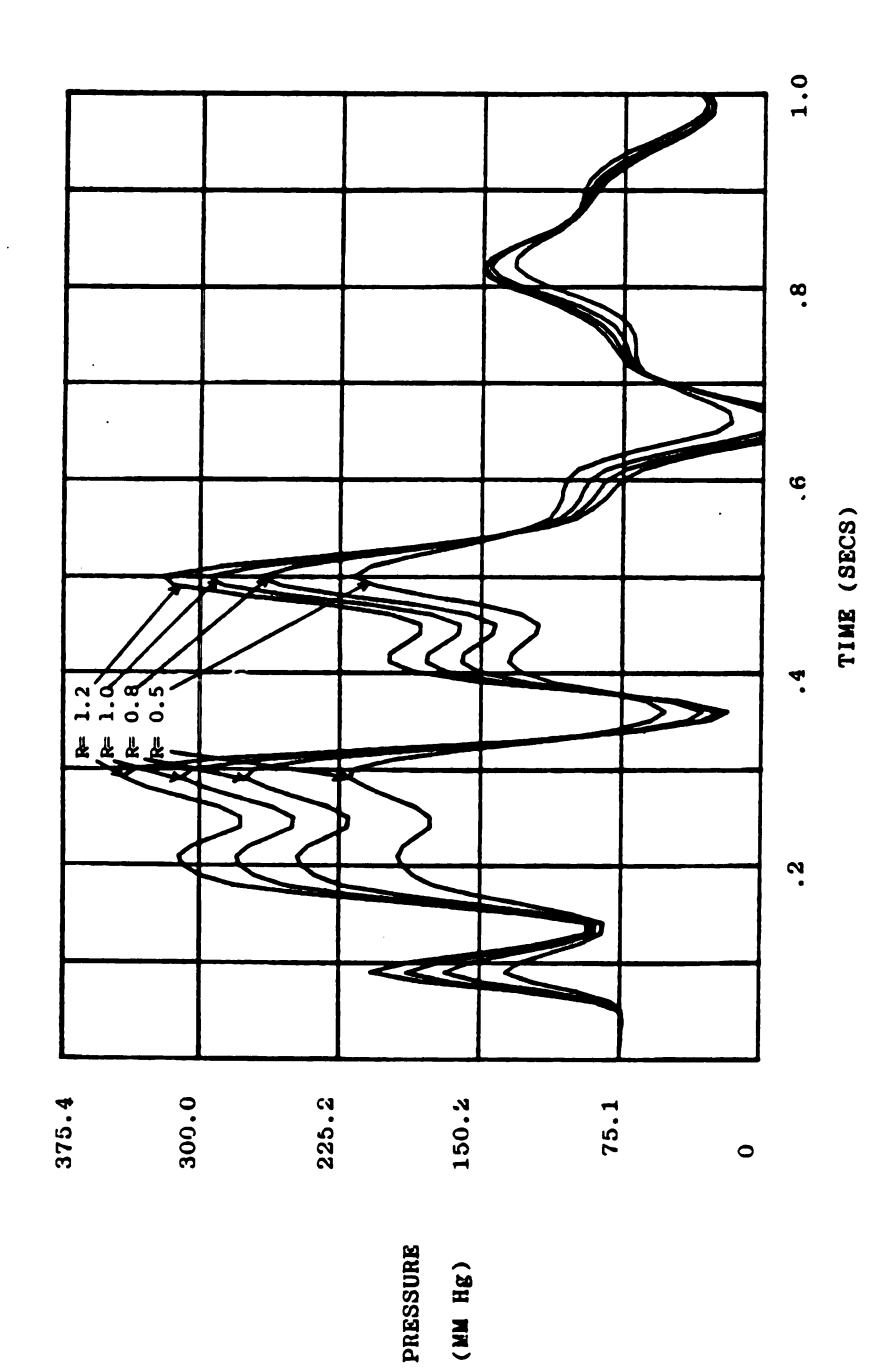
EFFECT OF CHANGING THE PATIENT'S COMPLIANCE

The value of the effective arterial compliance will vary of course from patient to patient due to the characteristics of the arterial walls for that person. Therefore this is a variable which must be accounted for. Another variable is the patient's peripheral resistance which can, in fact, change during the course of surgery (vasoconstriction), but in this case the pressure will simply be increased linearly (or decreased in the case of vasodilation) throughout the system. Therefore, only the effects of changing arterial compliance has been investigated in this thesis. Figure 6.20 demonstrates how increasing the arterial compliance from a control value of 0.5 cm⁴ s²/kg to 1.0 cm⁴ s²/kg causes decreased pressure peaks and smaller differences between "systolic" and "diastolic" pressures. The opposite is true for lower compliances. A compliance of 0.1 cm⁴ s²/kg causes very large pressures and large amplitude fluctuations.



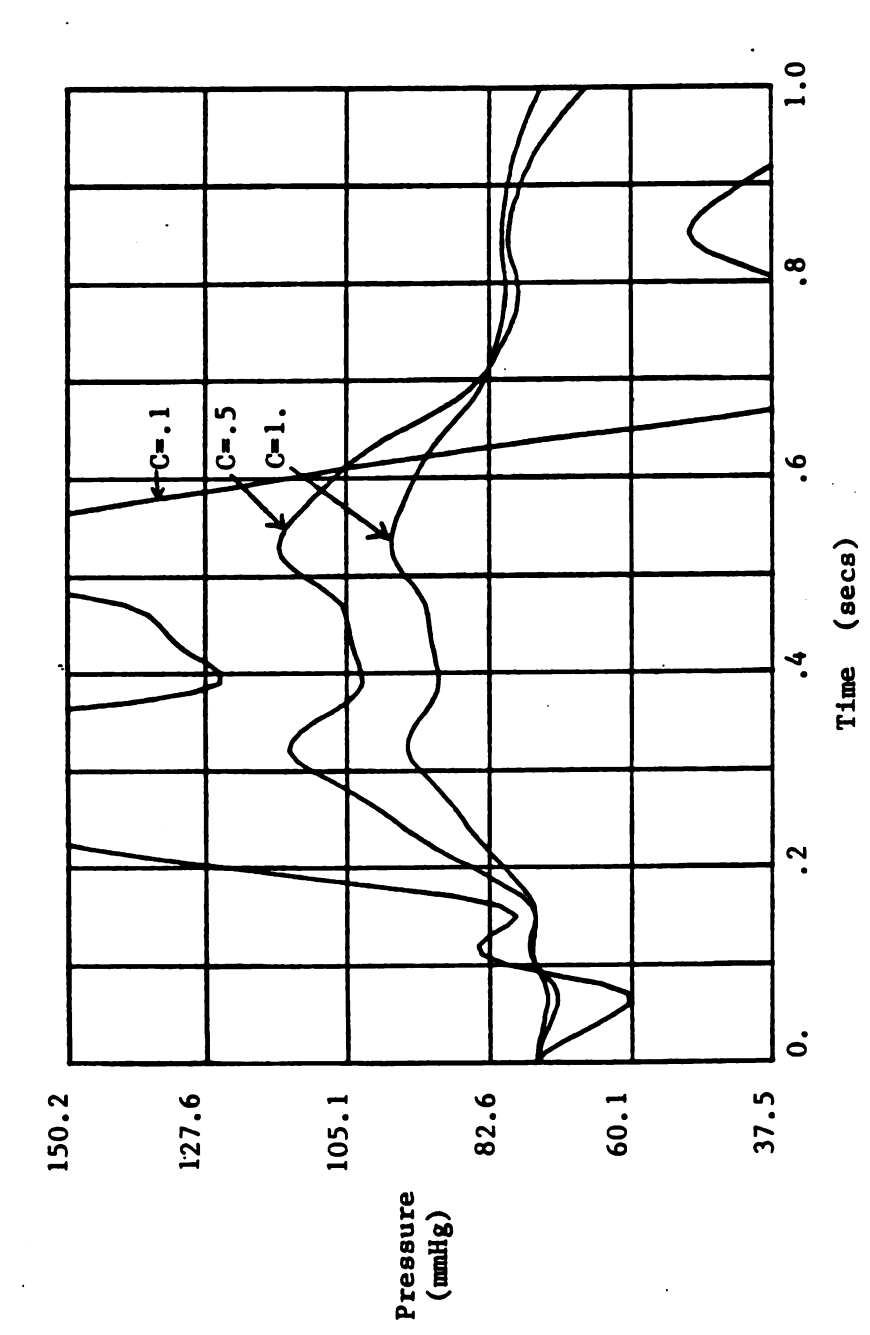
EFFECT OF CANNULA RESISTANCE ON AORTIC PRESSURE

Figure 6.18



EFFECT OF CANNULA RESISTANCE ON CANNULA PRESSURE

Figure 6.19



Effect of Patient's Arterial Compliance on Aortic Pressure

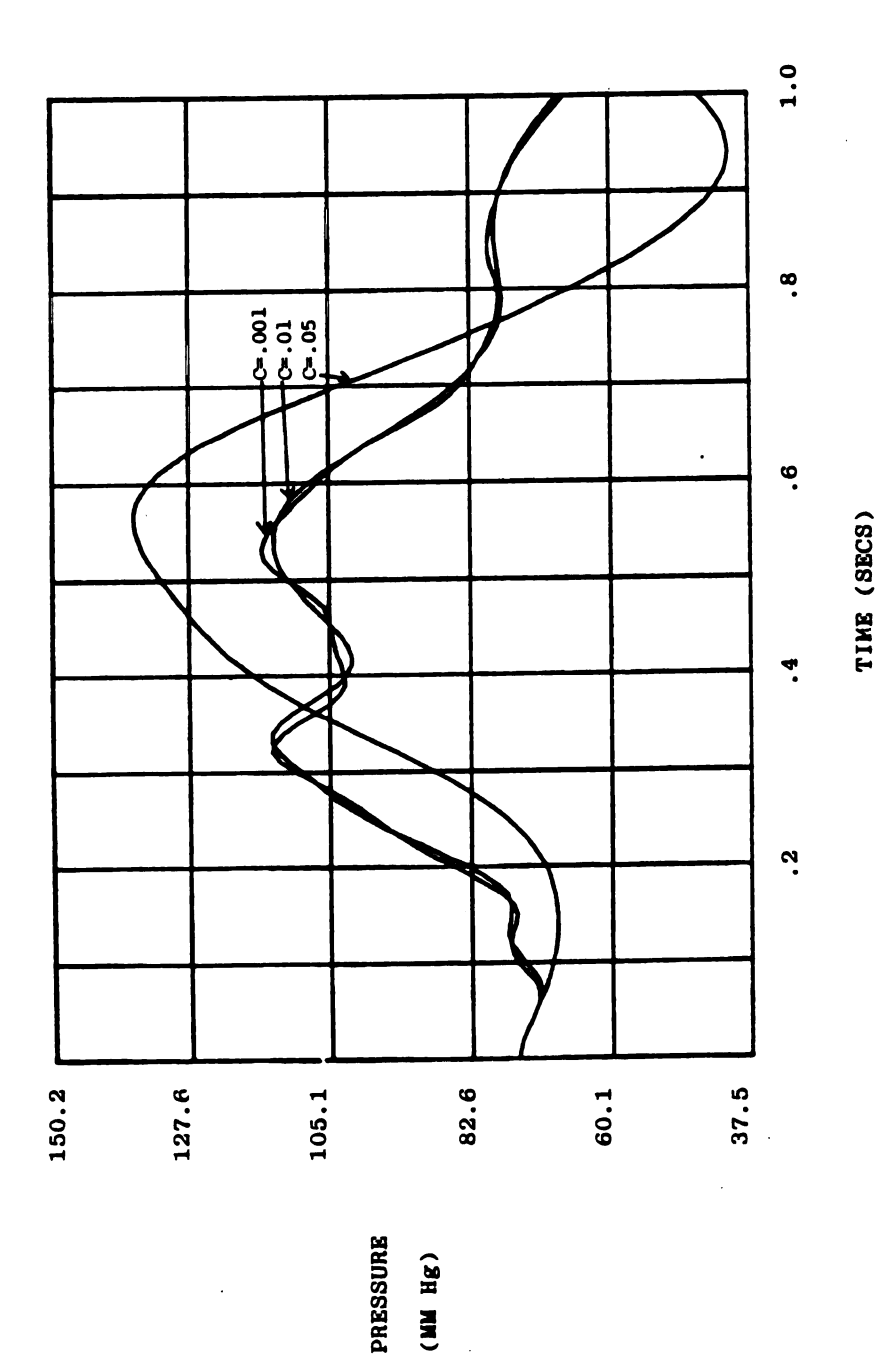
Figure 6.20

LOW PASS FILTERING

The final investigation involved determining methods of hydraulic filtering the pulsatile wave. The object was to pass only the low frequency component of the pressure wave and filter out the higher frequency components which resulted from rollers contacting and leaving the tubing in the header. In general, it is desirable to replicate as closely as possible the behavior of the biological system. It was theorized that the baroreceptors might sense the unnatural higher frequency components of the assist pulse and react in a detrimental fashion. Therefore, eliminating the roller artifacts was considered desirable.

There are two methods of low pass filtering. Either increasing the compliance or the inertia of the system will eliminate the higher frequency components of the pressure wave. In Figure 6.21 the capacitance of the system has been increased by increasing the value of the spring loaded accumulator. A subtle change is apparent when the accumulator compliance increases from 0.001 to 0.01 cm 4 s 2/kg. The system is spongier and, therefore, the pressure fluctuations are not as severe. However, when the compliance increases to 0.05 cm 4 s 2/kg there is definite filtering of the high frequency components. The pressure wave in this case is more sinusoidal which may or may not be an improvement.

Increasing the inertia of the system can be accomplished by lengthening the tube, increasing the fluid density, or decreasing the cross sectional area. Since the first two are going to be fixed in advance in most cases, the only way of increasing the inertia is to decrease the cross sectional area. An increase in the inertia of the



LOW PASS FILTERING WITH INCREASED ACCUMULATOR COMPLIANCE

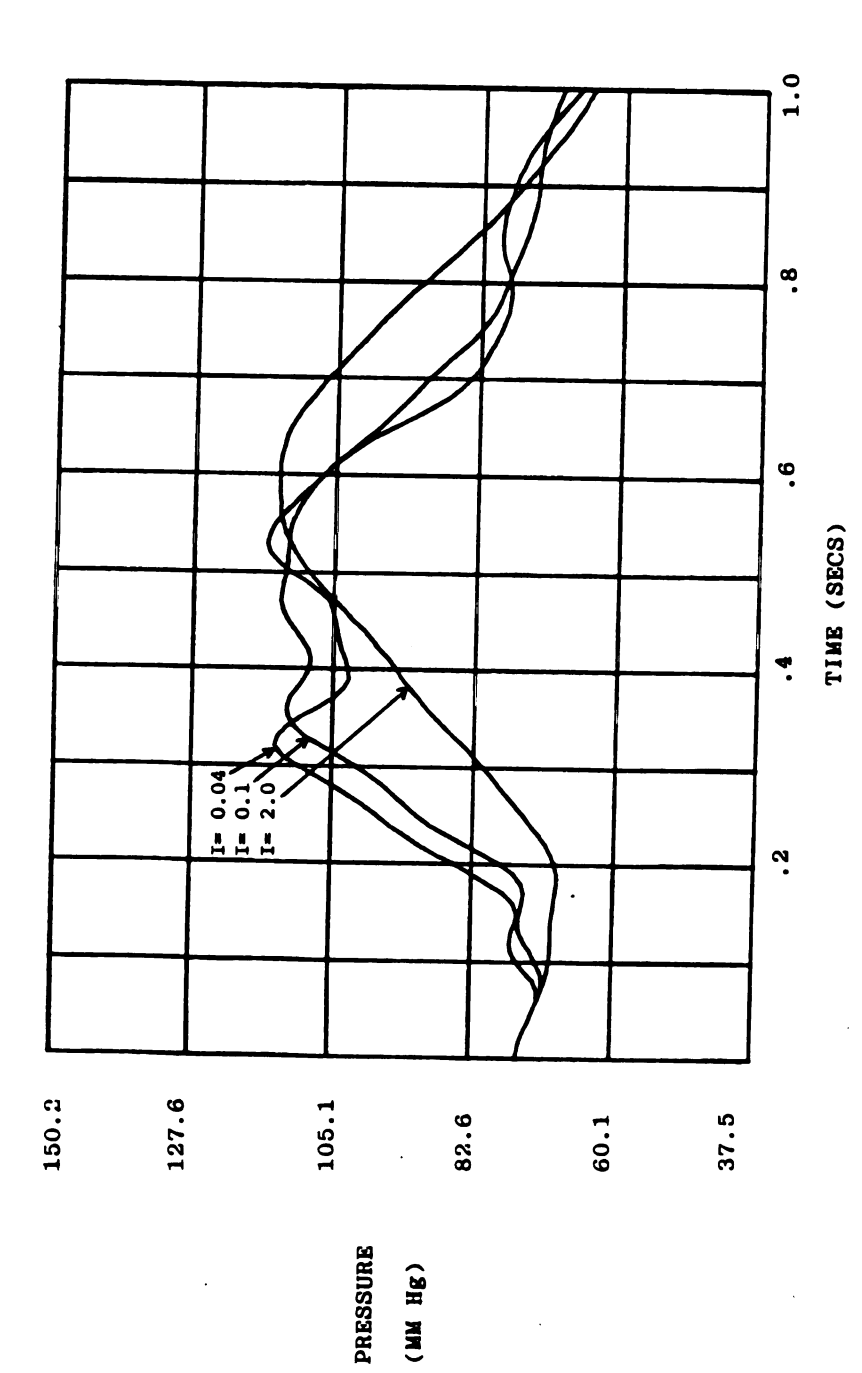
Figure 6.21

system is shown in Figure 6.22. Higher inertia values do effectively filter out the roller artifacts. Unfortunately a byproduct of the filtering is that the rising slope is much lower and may not be acceptable. In general, this method of filtering is not a viable option because decreasing the cross sectional area to induce a higher inertia would also cause a significant increase in the resistance to flow. This increase in the line resistance in the tubing would simply be unacceptable.

MANOMETER INACCURACIES DUE TO LINE INERTIA EFFECTS

In general most manometers must be physically located some distance away from the spot where the pressure measurement is desired. The conventional strain gauge monometer is connected to a length of small inner diameter tubing which is inserted into the radial artery in the arm of the patient. The tubing is generally fairly stiff to minimize compliance and resistance effects due to the wall of the tubing but the inertial increase which results from using small diameter tubing may significantly damp out much of the high frequency fluctuations. Just as the tubing was narrowed to increase the inertia of the system and filter out roller transients, the same effect is probably taking place with most manometer measurements. Thus the perfusionist may be unaware of the high frequency components of the arterial pressure wave. This section will document the size of tubing required to do the same amount of filtering which was previously found to eliminate all high frequency waves in the arterial system.

An inertia element of magnitude 2 kg/cm⁴ was found to act as an effective filter in the extracorporeal circuit. The tubing inner diameters and lengths which will cause the same effect are shown in



LOW PASS FILTERING WITH INCREASED INERTIA Figure 6.22

Table 6.5. The equation for the inertia as previously defined was:

$$I = p \mid 1$$

Since the density of the fluid (in this case water) is known to be 0.001 kg/cm^3 , the length and cross sectional area of the tube were varied to equal the inertia of 2.0 kg/cm^4 .

TABLE 6.5

TUBING LENGTHS AND AREAS RESULTING IN LOW PASS FILTER

ID	Length inches	Area cm ²	Inertia kg/cm ⁴
inches			
1/16	15.5	0.0198	2.
3/32	35.0	0.0445	2.
1/8	62.3	0.0792	2.
1/4	249.0	0.3168	2.

CHAPTER 7

DISCUSSION

Some of the conclusions which can be made from the preceding results will be summarized and discussed in this section.

Static compliances for tubing can be linearized over the range between 0-300 mmHg. The static compliances however cannot be used in any dynamic situation. This appears to be a result of the viscoelastic characteristics of the tubing wall which do not come into play in the slowly applied static test but will significantly retard the wall movement under dynamic conditions. There does not seem to be any significant nonlinearities associated with the tubing compliances under dynamic conditions although this was not evaluated very rigorously. In general, the Voigt model for the tubing wall seemed adequate to describe the contractile dynamic characteristics. One modification to this model would be to incorporate some sort of nonlinear resistance into the otherwise linear model. The resistive nonlinearities will be discussed later. The other difficulty was the lack of correlation between static and dynamic compliances. Although the static compliance seemed to approach the behavior of the measured tubing response with an increasing number of segments, there was still a discrepancy between measured and predicted response using the static compliance. Possibly this might be remedied by using a St. Venant body instead of a Voigt element. The ability of the St. Venant body to respond instantly to an applied load might improve the predictive response. Further research is required to better understand this.

The modelled wall resistance left more to be desired than the compliance characteristics. The combination of linearized entrance resistance, line friction, and wall resistance simply did not adequately describe the actual damping of the system. I am confident that the R values are within the approximate range estimated in the results section but the data was very crudely fit by the model. Figure 6.5 was the predicted response of three feet of tubing to a step pressure input. The resistance did not damp out the higher frequency components of the pressure wave. The actual response was much smoother. I found that by increasing the wall resistance values in the computer model, the output was smoothed out. Unfortunately, I was unable to acceptably fit the entrance resistance into a model that had the higher wall resistance values. Therefore, I would conclude that the wall resistance is probably higher than the value of 1.6 kg/cm but is nonlinear. If the resistance is parabolic or described by the equation:

$$P_1 - P_2 = R V_e^2$$

rather than the linearized resistance used, the high initial flows would experience very high resistance. After the system was settling around the equilibrium pressure of the reservoir, the flows would be of lower velocity and, therefore, would experience lower resistance. The resultant pressure wave would have significant damping of the first couple pressure peaks but less damping thereafter. It can therefore be concluded that linearizing the nonlinear resistances is not a good assumption in this model.

Another important conclusion about resistance effects is that wall damping appears to be much more significant than line friction losses.

This disputes Bergel's assumption that wall resistance in arteries could

neglected. This study was concerned with PVC tubing while Bergel concentrated solely on arterial walls but still the conclusion is important.

It was also important to be able to ascertain that temperature does not significantly affect viscous wall characteristics. There is a perceptible decrease in wall damping with a temperature rise from 20° to 37°C but the wall compliance appears to be unaffected. Since decreasing wall resistance did not significantly alter the aortic pressure, temperature changes will not significantly alter the aortic pressure. The wall resistance changes were not quantified but the qualitative effects were enough to see that the change in temperature during hypothermia would not substantially alter the patient's aortic pressure wave. If the compliance were affected by temperature, the natural frequency of the tubing would be altered, and thus, the carefully tuned system could be thrown off by hypothermia. The spring loaded accumulator would need be changed continuously with a fall or rise in temperature. The perfusionist should only expect an increased cannula pressure with decreased temperature but the arterial system will experience little change.

The high value of the entrance frictional effects was an unexpected result. The theoretical estimate of 0.0005 kg/cm⁴ was substantially less than my best fit estimate. The actual value was determined to be closer to 1.0 kg/cm⁴. I have a fair degree of confidence in the accuracy of this value (at least it is of the same order of magnitude) because the resistance should be approximately equal to the resistance of the cannula. The cannula resistance results from the sudden enlargement of the tubing from a cannula diameter to the much wider

aortic diameter. This sudden enlargement yields a resistance of about 1.2 kg/cm⁴. Entrance effects from the reservoir and the sudden enlargement from the tube back into the reservoir have similar flow characteristics: the abrupt change in geometry causes the fluid to neck down to a vena contracta as shown in Figure 7.1. The transition from the smallest area in the vena contracta to the diameter of the tube represents a significant frictional loss simply due to the sudden enlargement (a sudden enlargement is generally more resistive than a sudden contraction). This small cross sectional area in the vena contracta will experience high flow rates which can induce turbulence. All of these factors indicate that the transition from a large to a small area results in higher resistive losses than would be theoretically predicted.

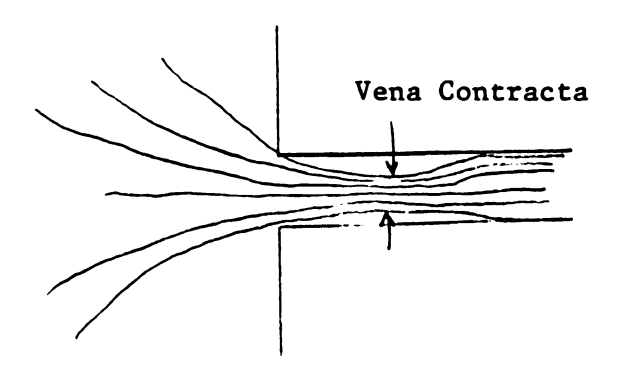


FIGURE 7.1

Vena Contracta from Area Change

I am emphasizing this as much as I am because there are numerous components of open heart surgery which have these sudden contractions or enlargements. Many oxygenators, filters and cannulae have no tapered

entrances and exits. Filters and cannulae have also been reported to induce high resistance to flow and can cause turbulence. These connections may not have been considered important during steady flow perfusion since the flow rates are generally fairly low but become much more significant with pulsatile flow with rapid flow acceleration and deceleration. Since Sarns is not presently in the oxygenator or filter business, taking these factors into account could yield several new disposable products which significantly improve the hemodynamics of extracorporeal circulation. Since Sarns presently manufactures and markets a line of cannulae, some design changes could significantly improve the performance of present products. A new cannula design is sketched out in Figure 7.2. Since a bell shaped funnel would significantly improve the flow characteristics of the device, this has been incorporated into the new design. The major problem is that since the cannula is inserted through the wall of the aorta it cannot have a very wide funneled exit because the wound would be too large. This problem has been remedied by a design which is inserted in a closed position but opens up when inside the aorta. The funnel would be made of a fairly stiff plastic which would be folded up like an umbrella. A noose would loop around the funnel which could be pulled to close up the funnel to facilitate insertion and removal. The cross sectional area of the widest part of the funnel would be less than that of the aorta so that the heart could still pump past the funnel during counterpulsation or before the heart is stopped. The flexible tube which would enclose the drawstring would open into the aorta.

The advantages of this new design would include:

 Less frictional resistance because the sudden enlargement would be eliminated.

PLEASE NOTE:

Page 74 is missing in numbering only as text follows.

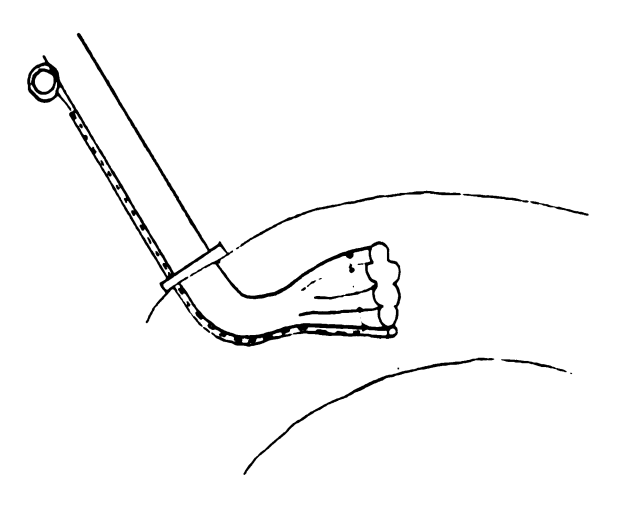


Figure 7.2

Cannula Design with Tapered Exit and Pursestring Removal

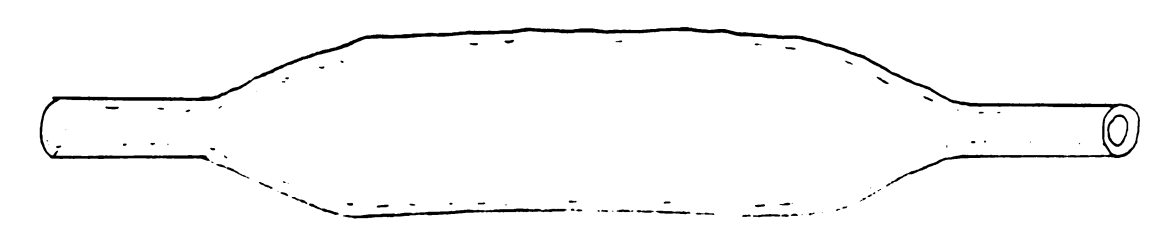


Figure 7.3

Extruded Header Tube with 3/4" ID Middle and 3/8" ID Ends

- 2) less turbulence because there would be no sudden enlargement to trigger turbulence. Also, there would not be the propagation of eddy wakes which must be present in the present cannula design. These eddies not only contribute to the overall friction of the device but additionally present dead spots where clotting can take place. Thrombosis will develop on any unwashed region in the circulatory system so a smooth funneled exit would experience little eddies and, therefore, little thrombus formation.
- 3) Pressures in the tubing upstream would be lower because of the reduced resistance of the cannula. The flow rate fluctuations would be also lower. Thus the peak velocities in the tube would be less and there would be less tubing losses. The incidence of turbulence in the tubing could also be diminished.

Turbulence has not been discussed in much detail in this report so I will briefly outline some of the problems incurred with turbulent flow. Turbulent flow is relatively rare in the normal cardiovascular system. Turbulent flow causes more shearing stresses in the flow than laminar flow. This is a problem because blood cells cannot withstand shearing stresses very well. Also, normal laminar flow in the arterial system is multilayered with the denser red and white blood cells carried along in the high speed flow in the center of the vessel. The periphery of the tube will have a thin radial layer of plasma. However, turbulence causes a great deal of mixing. This would disrupt the radial distribution of cells and plasma. More cells would be located towards the edge of the tube which experiences the greatest shearing stresses.

This would result in more hemolysis (destruction or lysing of the red blood cells) than in nonturbulent flow. Turbulence also causes increased resistance to flow. Therefore turbulent flow results in more resistance and more damage to the blood: both of which should be avoided if possible. Any design changes which would reduce the incidence of turbulence such as the cannula design or tapered entrances and exits to filters and oxygenators, should profoundly influence the hemodynamics.

Two methods of filtering out high frequency pressure fluctuations were demonstrated in the results section. Increasing the inertia of the tubing by decreasing the cross sectional area and increasing the compliance of the system with a variable compliance accumulator both filter out higher frequencies. This is advantageous because it more closely resembles the physiological characteristics of the pressure wave. Compliance filtering is far superior to inertial filtering because increasing the inertia from the initial value of 0.0428 kg/cm4 to 2.0 kg/cm 4 effectively filters the wave, but also causes an increase in the resistance. The inertia is inversely proportional to the square of the radius whereas the resistance is inversely proportional to the radius to the fourth power. Thus, decreasing the radius would cause the inertia to rise 48.7 times (2/0.0428) but would cause the resistance to rise 2,183.6 times. This increased resistance would be unacceptable. A better solution to the problem of increasing the momentum of the fluid might be to increase the volume flow rate by using a larger tube header. A new design is sketched in Figure 7.3. This extruded header can be manufactured by extruders with approximately the same wall thickness in the small and large tube segments. The piece would require no connectors which would restrict the flow and the transition from large to small diameters and vice versa would be very smooth. The major benefit of the header would be that it could eject much more fluid than a traditional 1/2" I.D. tube header. Thus, the average velocity of the fluid would be higher for a shorter time period; more like the actual heart. This is opposed to a 1/2" header which would have to make several roller passes to eject the same volume of fluid. If there were any backflow when the roller left the tube, a one way ball or butterfly valve could be included in the header.

A cantilever spring loaded accumulator could be used to tune the system. The cantilever spring could be of variable length so that simply by changing the length of the spring, the capacitance could be changed. Thus, the accumulator would permit variable capacitance for different patients. The capacitance value which effectively filtered out the high frequency roller pulses was found to be about 0.05 cm⁴s²/kg. The capacitance of a spring loaded accumulator is found by the equation:

$$C = A_c^3$$

where A_c is the area of capacitance and k is the spring constant. The size of the accumulator would need to be as small as possible to limit the amount of blood required to prime the system, therefore, a small accumulator with diameter of 4" would have an area of 81 cm². The spring constant needed for this would be about:

$$k = A_c/C = 81.0/0.05 = 1622 \text{ kg/cm}^2 \text{s}^2$$

Another method of capacitance would be to have a large tube bypassing the filter. There is normally a length of 3/8" I.D. tubing

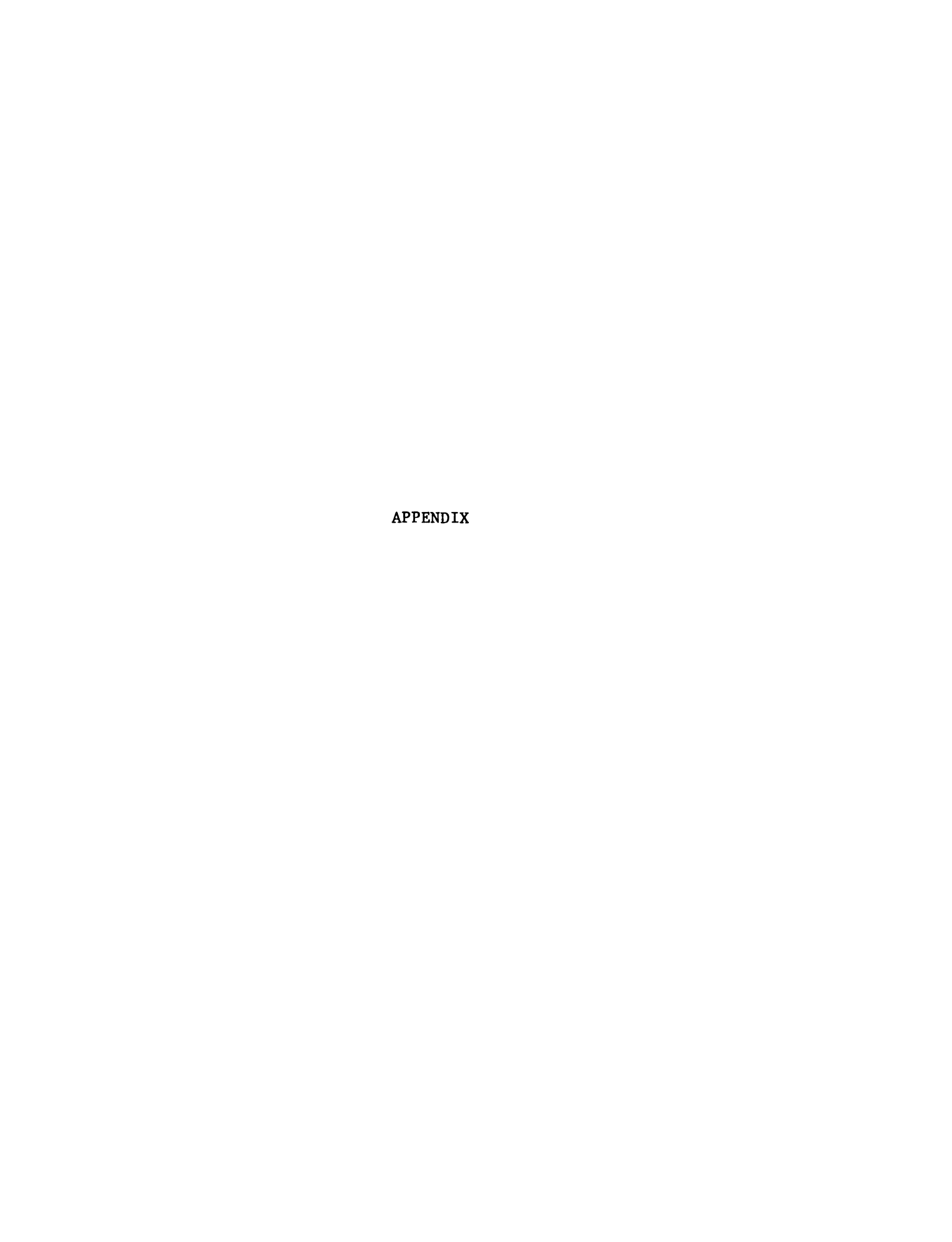
bypassing the filter in case of clogging, but this could be enlarged with a more flexible tube. By varying where the tube is clamped off the capacitance could be changed accordingly. The problem with this technique is that it would require a fair amount of blood to sit in a dead reagion, thereby increasing the amount of clotting and other problems associated with stagnant blood.

A small diameter tube used to connect the radial artery to the manometer would not require much tubing to effectively damp out much of the high frequency fluctuations. A 1/16" I.D. tube would only need to 15.5" long to eliminate all the high frequency pulsations in the pressure wave. Thus, perfusionists may not be aware of the actual characteristics of the pressure wave in the patient. This problem can be remedied by using larger diameter tubing.

The present model could be improved with some minor and some major changes. I believe that water is a fairly good blood analogue from an overall point of view. In other words, the two dimensional characteristics of the flow stream cannot be accurately modelled with water, but the gross effects including average velocity and pressure, can be fairly well estimated. However, the density of water is slightly less than that of blood. Using the higher density value in all the models would involve a minor change in the program. It was not done in this study because it was felt that the model is not accurate enough to detect changes as sensitive as this. Besides all testing was done with water. Additionally the viscosity and, therefore, the line resistance of blood is higher than water. This could be included in further models.

Further testing with a St. Venant body for the wall element might yield better results.

I would not recommend that anyone attempt to model the resistance of the cannula, tubing wall, line, or entrance/exit friction resistance with linear elements. A parabolic description of pressure vs. flow should yield better results.



APPENDIX A

A BRIEF REVIEW OF BOND GRAPH AND EIGENVALUE FORMULATION Bond graphs are a useful tool in determining the state differential equations of a system composed of storage elements; capacitance and inertia elements. A bond graph can be thought of as a shorthand representation of a system much like a free body diagram can be used to find the equations for a mechanical system. It is particularly useful because a bond graph can be used to determine the state equations in many otherwise unrelated engineering disciplines such as mechanics, hydraulics, electrical and thermal systems. Because this methodology may be unfamiliar to some readers, a brief review will be presented with the final object of being able to visualize how the differential equations can be found easily given the bond graph. Enport 5 is a computer program capable of accepting bond graphs directly and will construct the state equations if the parameters are known. Therefore in many instances the bond graph of a complex system will be presented without the corresponding state equations.

Once the state equations have been derived and put in matrix form, it is a relatively straight forward procedure to find the eigenvalues of the system. The eigenvalues are equivalent to the square of the natural frequency of a system which will be of great interest in this project. The determination of eigenvalues given system state equations will be shown in a simple example.

Given a simple spring, mass, damper system sketched in Figure A.1, the state equations describing the motion can be found by

- circuit analysis
- free body diagrams

- Lagrangian analysis
- bond graphs

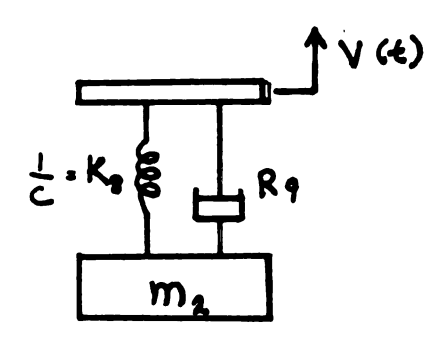


FIGURE A.1

Mechanical Oscillator

All components of bond graph systems are made up of power variables. Two energy variables effort and flow, are common to all systems and the product of the two is the power flowing through the bond. For example an electrical bond has energy variables voltage and current and the product of the two gives the power in watts. Table A.1 shows the energy variables effort and flow, for several domains.

TABLE A.1
Energy Variables for Various Domains

Domain	Effort	Flow
Mechanical translation	Force (N. or 1bf)	Velocity (m/s or ft/s)
Mechanical rotation	Torque (Nm or ft 1bf)	Ang. vel. (rad/s, rpm)
Hydraulic	Pressure (N/m², psi)	Vol. flow rt.(1/s, ft ³ /s)
Electrical	Voltage (volts)	Current (Amperes)

TABLE A.2

One Port Variables for Various Domains

Device	Hydraulic	Mechanical	Electrical
Resistor	Friction in pipe	Couloumb friction	Resistor
	Valve	Dashpot (viscous)	
→ R	Wall damping	Bearing friction	
	Sudden contraction		
	T junction, etc.		
Capacitor	Tube flexibilities	Spring	Capacitor
	Fluid compression	Tires on vehicle	
 c	Spring loaded		
	accumulator		
	Gravity field		
	(storage tank)		
Inertance	Fluid mass	Mass of solid object	Inductor
I		or moment of	
		inertia	

One Port Variables

Bond graphs are comprised of three basic elements which experience power entering through only one port. These elements alter either the effort or flow by dissipating or storing energy.

Table A.2 shows some specific examples of one port variables in several domains. In many cases these are idealized mathematical versions of the real devices. The bond graph symbol for each of them is also shown. The resistor will dissipate energy while the capacitance and inertance elements will both store energy. Each storage element will have a unique state variable and state equation. Power always flows into these devices, hence an arrow pointing at the element is shown in Table A.2. Another type of one port variable alters the power by inputting a source of effort or flow into the system. These source elements model physical devices such as pumps, motors, batteries, etc. They are defined so that power always flows away from the elements so their bond graph symbol has the arrow pointing away as shown in Figure A.2

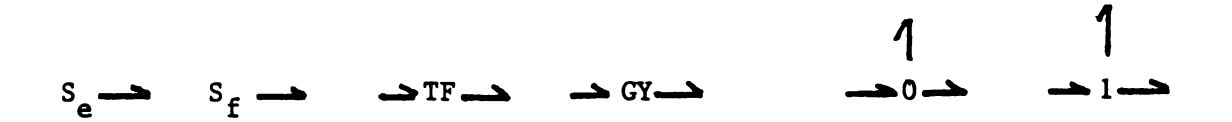


FIGURE A.2 FIGURE A.3

Sources and Transformers Junctions

Two Port Elements

Power is conserved when passing through a two port element as opposed to being dissipated, stored, or generated in one port elements. The two types of two port elements are the transformer and gyrator. The transformer transforms or scales effort to a scaled effort and flow to a scaled flow. A electrical transformer, a lever, and a hydraulic ram are examples of transformers in various domains. An ideal transformer will have the following constitutive laws:

$$e_1 = m e_2$$
 EQN. A.1
 $m f_1 = f_2$ EQN. A.2

where m is the modulus of transformation. A gyrator will transform an effort into a scaled flow and vice versa. The constitutive laws for this device are:

$$e_1 = r f_2$$
 EQN. A.3
 $f_1 r = e_2$ EQN. A.4

The schematic representation for both are included in Figure A.2

Multi Port Junction Elements

Two junction elements are used to connect the one and two port elements together. A common flow junction is represented by a 1 with several bonds extending from it. A common effort uses a 0 instead of a 1. A common flow (which will be hereon referred to as a 1-junction) requires that the flow through all the elements in the junction be common such as in a series of electrical elements. The effort will sum in such a junction. Conversely a common effort junction (which will be called a 0-junction) can be likened to a parallel combination of electrical elements and the flow will sum through this junction. Bond graph schematics for the two junctions are shown in Figure A.3.

Model Building

The procedure for constructing the model from the various elements previously described requires the following rules.

- 1) For a mechanical system, identify unique velocities such as a mass with a unique velocity or a velocity source. For the hydraulic or electrical case, unique efforts (pressures or voltages) are easier to identify. Put a zero with each effort and a one with a unique flow.
- 2) Identify a reference ground. Usually this will have no velocity or atmospheric pressure. Label this with the appropriate one or zero.
- 3) All elements in the mechanical domain which store or dissipate power connect to 0-junctions. In other domains all of these elements connect to 1-junctions.
- 4) Attach sources to the appropriate junctions. The source of effort associated with the gravity of a block, for example, would be attached to the 1-junction associated with the mass of the block.
- 5) Once all elements are connected, the reference can be eliminated along with all bonds attached to it.
- 6) 0- and 1-junctions with only two ports can be eliminated since they are performing no function.
- 7) Power is assigned by the rules
 - power flows out of sources;
 - power flows into R, C, and I elements;
 - power flows away from the source which is driving the system through. This applies to junctions.

EXAMPLES

A couple of examples will illuminate these rules as applied to the mechanical and hydraulic domains. First, the bond graph for the spring, mass, and damper system shown in Figure A.1 is started by identifying unique velocities. There is one unique velocity associated with the mass and another associated with the velocity driver. A third velocity is ground and will be zero. The spring and damper (C and R elements) attach to zero junctions between the first two velocities. The inertia attaches to a zero junction between the one junctions corresponding to the velocity of the mass and ground. Next sources are added to the bond graph. The source of effort associated with gravity is attached to the 1 junction associated with the mass velocity. A source of flow is connected to the second 1-junction. At this point all elements have been connected so the ground in eliminated with its bonds. This would leave the I element connected to a 0-junction with only two ports so the zero can be neglected. The resulting bond graph is shown in Figure A.4.

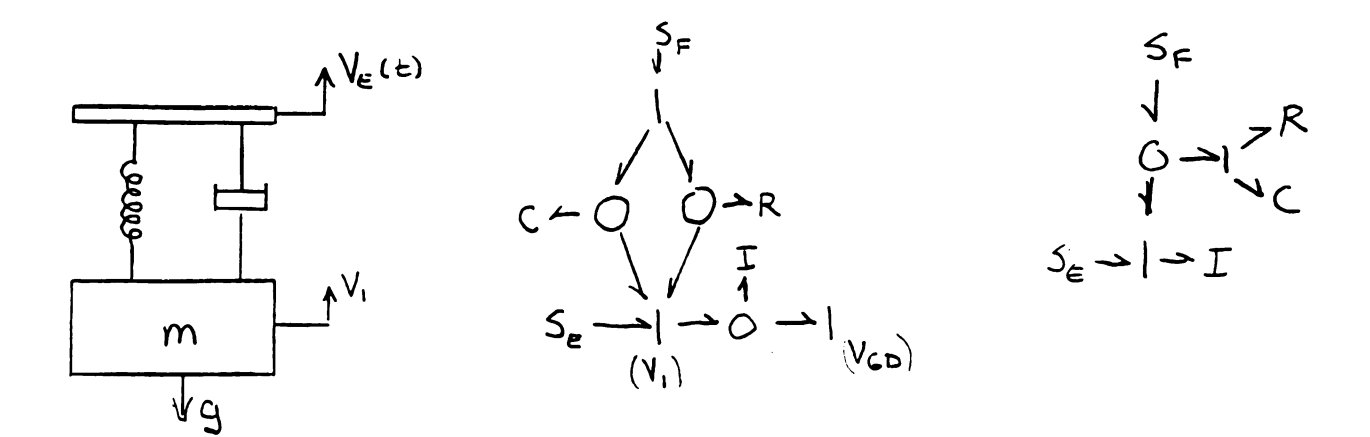


FIGURE A.4
Oscillator Bond Graphs

An equivalent bond graph is also shown in which the C and R elements have been consolidated. If one considers the physics, this simplification can be rationalized. The spring and the damper will have the same velocity unless there is some sort of rotational motion. Since this is not the case it can be seen that connecting the R and C to a l-junction is justified. The flow which the spring and damper mutually feel is caused by both the flow source and the velocity of the mass. This is represented by the flows adding at the 0-junction. Since this simplification would leave a one junction connected only to a zero and a source of effort, making it a two port, it also can be eliminated leaving the final bond graph in Figure A.4.

The second example represents one of the experiments designed to evaluate the spring and damping characteristics of the Voigt element. A length of tubing is pressurized and connected to a reservoir. The tubing is clamped off and the reservoir is pressurized to a higher level. Releasing the clamp will effect a pressure step input to the tube or a source of effort. The diagram of the experiment and the bond graph is shown in Figures A.5 and A.6. The bond graph formulation is started by identifying two unique pressure points; one in the reservoir and the other at the end of the tube where the pressure is measured. A third pressure is identified as atmospheric and this will be the ground for the system.

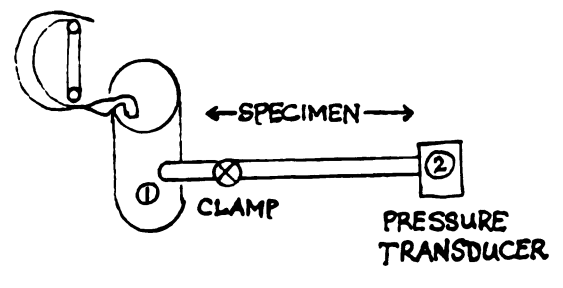


FIGURE A.5

Step Input Test Setup

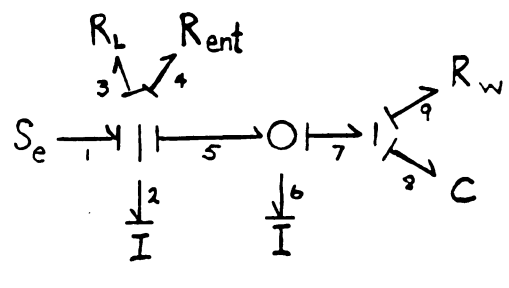


FIGURE A.6

Simplified Bond Graph

Between the reservoir and the end of the tube can be inserted line inertia, the resistance due to viscous shearing known as line resistance from now on, and the resistance due to the entrance effects. Since these are all effectively the same volume flow rate, all can be included on the same l-junction. The capacitance and resistance due to the wall are connected to l-junctions between the downstream pressure and atmospheric. This l-junction is the wall velocity so the two can be combined in a similar manner as that defined for the mechanical example. Figure A.6 show the initial and simplified bond graphs.

CAUSALITY

The objective of the bond graph is to aid in developing the differential equations which describe the systems behavior. The elements in the spring, mass, damper example will interact with one another: the momentum of the mass will affect the relative velocity of the spring while the spring exerts a force on the mass. In order to relate the state variables, causality must be included in the bond graph. As previously described, a 0-junction will have a common effort which must come from one of the bonds. In essence this is saying that one of the bonds is causing the effort or flow on a 0- or 1-junction respectively. For example a velocity source on a 1-junction is the cause of the flow. The inertia of a mass will be the cause of flow at a 1-junction unless it is overridden by a velocity source. The rather abstract concept of causality will help in tracing the effect of sources and other state variables on the dynamics of a state variable. Causality is represented graphically by a small stroke perpendicular to the bond. If the causality induces a flow on a bond then the stroke is away from the junction while effort causality is symbolized by the

stroke next to the junction. The causality is fixed for effort and flow sources so they can illustrate the causal strokes (see Figure A.7). Inductors and capacitors have preferred causality as shown in Figure A.7. Preferred causality means that unless the causality is overridden by a source, this is the causality on the element. Resistors have no preferred causality nor do transformers or gyrators. The only requirement that 0- and 1-junctions have is that there is only one effort stroke on a 0-junction and only one flow stroke on a 1-junction (see Figure A.7).

The concept of causality can be understood better with an understanding of the consitutive laws of the element. Table A.3 lists consitutive laws for the various elements in different domains.

. Preferred Causality of Elements and Junctions

From the table, a compliance element with a given volume has a fixed pressure. A spring with a fixed elongation has a force and a capacitor with a charge will have a voltage difference between the plates of the capacitor. In terms of causality this is saying that a compliance unit with preferred causality will impose an effort on a junction. Similarly an inertance element will impose a flow on a junction. A resistor will impose either a flow or effort depending on the causality resulting from the rest of the system.

TABLE A.3

Constitutive Equations for Various Elements

	HYDRAULIC	MECHANICAL	ELECTRICAL
С	P = 1/C V	F = 1/C X	$E = 1/C Q_e$
I	Q = 1/I L	$X = 1/m P_m$	i = 1/I g
R	P = R Q	F = R X	E = R i

(Note: V is volume, P pressure, F force, X displacement, E voltage, Q charge, Q volume flow rate, L momentum slug, m mass, P momentum, i current, g flux linkage, X velocity.)

Causality rules follow:

- 1) First assign causality to all sources.
- 2) If source causality does not impose causality on the rest of the junction, next assign causality to C and I elements.
- Assign causality to R elements not already constrained by the causality of the rest of the system. If it makes no difference which way causality is assigned, then just choose a causality.

Going back to the bond graph for the hydraulic case, causality is initially assigned to the effort source. Next causality can be established for the storage elements. Assigning flow causality to the inertance element means that this bond is the flow source for the 1-junction and all others must be effort bonds. The causality for the other elements are forced by this action.

A previously unmentioned element is now introduced; the activated bond. An activated bond is a bond graph pressure tap or flow meter. It

allows examination of the pressure on a 0-junction or flow on a l-junction without changing the system dynamics. In the case of the hydraulic bond graph, the pressure at the 0-junction can be found by activating an inertia element. Activation is defined to mean that an inertia element will contribute no flow to the system while a capacitor will induce no effort. These are the only bonds which can be activated. The derivative of the activated bonds state variable will be the effort (for an I element) or the flow (for a C element). The hydraulic system with a complete bond graph is shown in Figure A.8.

FIGURE A.8

Hydraulic Bond Graph with Causality

THE DIFFERENTIAL EQUATIONS

The differential equations can now be found by tracing the causality through the system until the differential equations are functions only of state variables or sources. The procedure can be demonstrated with the hydraulic system. There are three storage elements with state variables L_2 , L_6 , and V_8 , therefore, there will be three state equations. Starting with L_2 the causality of the 1-junction means that the derivative of the slug momentum which is the

pressure, comes from the efforts on bonds 1, 3, 4, and 5. Or in equation form:

$$\dot{L}_2 = e_1 - e_3 - e_4 - e_5$$
 EQN. A.5

(minus signs are because power is flowing away). The effort on bond one, however, is simply the source of effort. The effort on bonds 3 and 4 is R times the flow in the bond and the effort from bond 5 comes from the effort junction and therefore derives from bond 7. Thus,

$$L_2 = S_e - R_3 f_3 - R_4 f_4 - e_7$$
 EQN. A.6

But the flows in junctions 3 and 4 are common to the flow coming from the I element (the causal stroke indicates that I_2 is causing the flow at that junction). By the constitutive laws for the I element:

$$f_3 = f_4 = 1/I L_2$$

Since this now is in terms of a state variable, we can turn our attention to the effort in bond seven. This effort is the sum of the efforts in bonds eight and nine. The effort in bond eight is found with the constitutive law for a capacitor and the effort in bond nine is again the resistance times the flow in the bond. Therefore,

$$e_7 = 1/C V_8 + R_9 f_9$$

Only f_9 remains to be traced back to sources and state variables. f_9 is equivalent to f_7 which is the sum of flows f_5 and f_6 . But since bond six is an activated bond it will not contribute a flow to the junction. And the flow in bond five is the same as that in bond two:

$$f_5 = f_2 = 1/I L_2$$

This can be inserted into the equation for e₇ giving:

$$e_7 = 1/C V_8 + R_9/I_2 L_2$$

The complete expression for the derivative of L_2 is now

$$\dot{L}_2 = S_e - (R_3 + R_4 + R_9)/I_2 L_2 - 1/C V_8$$
 EQN. A.7

The other two state variables are easier to trace. The volume flow rate in bond eight is:

$$Q_8 = f_7 = f_5 = f_2 = 1/I_2 L_2$$
 EQN. A.8

The state equation for bond six is:

$$L_6 = e_7 = 1/C V_8 + R_9/I_2 L_2$$
 EQN. A.9

Equations A.7-A.9 are the state equations describing the behavior of the hydraulic system. These equations can be put into matrix form to yield:

$$\frac{d}{dt} \begin{cases} L_2 \\ L_6 \\ v_8 \end{cases} = \begin{cases} (R_3 + R_4 + R_9)/I_2 & 0 & -1/C \\ R_9/I_2 & 0 & 1/C \\ 1/I_2 & 0 & 0 \end{cases} V_8 \begin{pmatrix} 1 \\ 0 \\ 0 \\ 0 \end{pmatrix} S_e$$

A Matrix

B Matrix

The eigenvalues for this system (W) are found by subtracting the matrix:

0 0 W

from matrix A and finding the roots of the determinant. The resulting

characteristics equation is:

$$-W^3 - (R_3 + R_4 + R_9)/I_2 W^2 + 1/(I C) W = 0$$
 EQN A.10

The roots of this equation can be determined by realizing that one of the roots is zero ($W_3 = 0$) and finding the other two with the quadratic formula:

$$W_{1,2} = -\frac{(R_3 + R_4 + R_9)}{2 I_2} \pm \sqrt{\frac{(R_3 + R_4 + R_9)^2}{2 I_2}} - \frac{1}{I_2 C}$$
EQN. A.11

The natural frequency is W^2 and can be approximated from equation A.10 by:

$$w_n = W^2 = \sqrt{\frac{1}{I C}}$$
 EQN. A.12

This system will be underdamped if the radical in equation A.ll is complex; that is the value under the radical sign is negative. The system will be critically damped at the point where the radical is equal to zero. Therefore, the critical damping for this simple system is when:

$$\left(\frac{R_3 + R_4 + R_9}{2 I_2}\right)^2 = 1$$

$$I_2 C$$
EQN. A.13

This information will be very useful in predicting the natural frequency of a single lumped parameter model of a length of tubing with known parameters I, C, R_3 (entrance effects), R_4 (viscous line looses). R_9 is the resistance due to wall damping and this variable can be solved to determine approximately what damping would be required to critically damp the system.

BIBLIOGRAPHY

- Angell-James J E and de Burgh Daly M. "Effects of Graded Pulsatile Pressure on the Reflex Vasomotor Responses Elicited by Changes of Mean Pressure in the Perfused Carotic Sinus-Aortic Arch Regions of the Dog." <u>J Physiol</u> 1971; 214: 51
- 2. Bergel D.H. "The Dynamic Elastic Properties of the Arterial Wall." J Physiol 1961; 156: 458-469
- 3. Brewer J W. Control Systems 1974 Prentice-Hall, Inc. New Jersey
- 4. Burton A C. "Relation of Structure to Function of the Tissues of the Wall of Blood Vessels." Physiol Rev 1954; 34: 618
- 5. Clarke C P, Kahn D R, Dufek J H, Sloan H. "The Effects of Nonpulsatile Blood Flow on Canine Lungs." Ann Thorac Surg 1968; 6: 450
- 6. Cronston R C, Rummel J A, Kay F J. "Computer Model of Cardiovascular Control System Responses to Exercise." J Dyn Sys Meas Con; Sept 1973: 301-307
- 7. The Exchanger; Sarns publication, 6200 Jackson Rd., Ann Arbor, MI 48106; Dec. 1968
- 8. Galletti P M, Brecher G A. <u>Heart Lung Bypass Principles and Techniques of Extracorporeal Circulation</u>, 1962 Grune & Stratton, New York, NY
- 9. Heart Facts; American Heart Association, 1983
- 10. Landymore R W, Murphy D A, Kinley C E, et al. "Does Pulsatile Flow Influence the Incidence of Postoperative Hypertension?" Ann Thorac Surg 1979; 28: 261
- 11. Mandelbaum I & Burns W N. "Pulsatile and Nonpulsatile Blood Flow." JAMA 1965; 191: 657
- 12. Mandelbaum I, Berry J, Silbert M, et al. "Regional Blood Flow During Pulsatile and Nonpulsatile Perfusion." Arch Surg 1965; 91: 771
- 13. Mase G E. Theory and Problems of Continum Mechanics; 1970 Schaum's Outline Series, McGraw-Hill New York, NY
- 14. Mavroudis C. "To Pulse or not to Pulse." Ann Thor Surg 1978; 25: 259
- 15. McDonald D A. Blood Flow in Arteries; Edward Arnold, London; 1974
- 16. Parsons R U & McMasters P D. "The Effect of the Pulse on the Formation and Flow of Lymph." J Exp Med 1938; 68: 353
- 17. Pfaender L M. "Hemodynamics in the Extracorporeal Aortic Cannula: Review of Factors Affecting Choice of the Appropriate Size." Emory University School of Medicine, Atlanta, GA

- 18. Reed C C & Clark D K. Cardiopulmonary Perfusion; Texas Medical Press, Houston, TX; 1975
- 19. Rosenberg G, et al. "Design and Evaluation of the Pennsylvania State University Mock Circulatory System." ASAIO J 1981; April/June: 41-49
- 20. Rosenberg R C. Class notes for ME 851: Modelling of Mechanical Systems; Michigan State University, East Lansing, MI 48823; 1982.
- 21. Shepared R B, Simpson D C & Sharp J. "Energy Equivalent Pressure." Arch Surg 1966; 93: 730
- 22. Snyder M F & Rideout V C. "Computer Modelling of the Human Systemic Arterial Tree." J Biomech 1968; 1: 341-353
- 23. Soroff M S, et al. "Hemodynamic Effects of Pulsatile and Nonpulsatile Blood Flow." Arch Surg 1969; 98: 321
- 24. Taylor M G. "An Experimental Determination of the Propogation of Fluid Oscillations in a Tube with a Visco-Elastic Wall together with an Analysis of the Characteristics Required in an Electrical Analogue." Phys Med Biol 1959; 4: 63-82
- 25. Taylor K M, et al. "Peripheral Vascular Resistance and Angiotensin II Levels During Pulsatile and Nonpulsatile Cardiopulomnary Bypass." <u>Thorax</u> 1979; 34: 594
- 26. Thompson W T. Theory of Vibrations with Applications Prentice-Hall, Inc., Englewood Cliffs, NJ; 1972
- 27. Vander A J, Sherman J H, Luciano D S. <u>Human Physiology the</u>
 Mechanisms of Body Functions McGraw-Hill Co., New York, NY; 1975
- 28. Watkins W D, Peterson M B, Kong D L, et al. "Thromboxane and Prostacyclin Changes During Cardiopulmonary Bypass With and Without Pulsatile Flow." J Thor Cardiovas Surg 1982; 84: 250
- 29. Westerhof N & Noordergraff A. "Arterial Viscoelasticity: A Generalized Model." J Biomech 1970; 3: 357-379